© 2020. Published by The Company of Biologists Ltd | Development (2020) 147, dev188730. doi:10.1242/dev.188730

RESEARCH ARTICLE

Pou2f1 and Pou2f2 cooperate to control the timing of cone photoreceptor production in the developing mouse retina

Awais Javed[1,2], Pierre Mattar[1,*], Suying Lu[3], Kamil Kruczek[4,‡], Magdalena Kloc[4], Anai Gonzalez-Cordero[4,§], Rod Bremner[3], Robin R. Ali[4,5] and Michel Cayouette[1,2,6,7,¶]

ABSTRACT

Multipotent retinal progenitor cells (RPCs) generate various cell types in a precise chronological order, but how exactly cone photoreceptor production is restricted to early stages remains unclear. Here, we show that the POU-homeodomain factors Pou2f1/Pou2f2, the homologs of *Drosophila* temporal identity factors nub/pdm2, regulate the timely production of cones in mice. Forcing sustained expression of Pou2f1 or Pou2f2 in RPCs expands the period of cone production, whereas misexpression in late-stage RPCs triggers ectopic cone production at the expense of late-born fates. Mechanistically, we report that Pou2f1 induces Pou2f2 expression, which binds to a POU motif in the promoter of the rod-inducing factor *Nrl* to repress its expression. Conversely, conditional inactivation of Pou2f2 in RPCs increases Nrl expression and reduces cone production. Finally, we provide evidence that Pou2f1 is part of a cross-regulatory cascade with the other temporal identity factors Ikzf1 and Casz1. These results uncover Pou2f1/2 as regulators of the temporal window for cone genesis and, given their widespread expression in the nervous system, raise the possibility of a general role in temporal patterning.

This article has an associated 'The people behind the papers' interview.

KEY WORDS: Cell fate, Mouse, Photoreceptors, Retina, Temporal patterning, Transcription

INTRODUCTION

The generation of neuronal diversity is crucial to building a functional nervous system. Classical studies have shown that, in some regions of the nervous system, the spatial position of neural progenitors is key to engage transcriptional regulatory networks that induce a particular fate (Jessell, 2000). In other regions, developmental time is used to diversify the progenitor pool (Ebisuya and Briscoe, 2018; Kohwi and Doe, 2013). A particularly striking example of such 'temporal patterning' is observed in the developing vertebrate retina, where the temporal identity of multipotent retinal progenitor cells (RPCs) changes progressively, such that their competence to give rise to different retinal cell types is altered as a function of developmental stage. Ganglion, horizontal, amacrine and cone photoreceptor cells are generally born early, whereas rod, bipolar and Müller glial cells are generally born late (Rapaport et al., 2004; Young, 1985a,b; Carter-Dawson and LaVail, 1979a,b; Turner et al., 1990). Although much is known about the transcriptional networks operating to instruct the generation of various cell fates available to RPCs within a given temporal window (Bassett and Wallace, 2012), much less is known about how these differentiation programs are activated at the appropriate time to control cell birth order.

Changing environmental signals in the developing retina contribute to alter RPC cell fate potential (Ma et al., 2007; Ozawa et al., 2007; Kim et al., 2005), but these cues act as inhibitory signals for specific cell types rather than as instructive cues, and heterochronic grafting studies have shown that the environment is not sufficient to alter fate output (Cepko, 1999; Belliveau and Cepko, 1999; Watanabe and Raff, 1990). Moreover, the size and composition of clones produced in clonal-density cultures are indistinguishable from those of clones produced *in situ* and the general order of cell birth is maintained in such cultures (Cayouette et al., 2003; Gomes et al., 2011). Thus, cell-intrinsic programs largely appear to control temporal identity transitions in RPCs. But what could these intrinsic factors be? A clue was provided by pioneering studies of *Drosophila* neuroblasts. In these lineages, the transcription factors hunchback (Hb), krüppel (Kr), Nub/Pdm2 (collectively called Pdm) and castor (Cas) are part of a temporal identity cascade where each factor is necessary and sufficient for the generation of neurons born during the temporal window in which they are expressed (Isshiki et al., 2001; Kambadur et al., 1998; Brody and Odenwald, 2000; Grosskortenhaus et al., 2005; Pearson and Doe, 2003; Novotny et al., 2002; Grosskortenhaus et al., 2006; Cleary and Doe, 2006). This cascade is tightly controlled by feedforward and feedback loops operating to restrict the expression of each temporal factor in its respective expression window (Doe, 2017). More recently, other temporal identity factors have been identified in different lineages of the fly nervous system (Li et al., 2013; Suzuki et al., 2013; Erclik et al., 2017), suggesting that such cascades might represent a general strategy to regulate progenitor competence.

Previously, we showed that mouse Ikzf1 (also known as Ikaros) is orthologous to *Drosophila* Hb and confers early temporal identity in RPCs, allowing production of three of the early born retinal cell types: ganglion, horizontal and amacrine (Elliott et al., 2008). Conversely, we showed that mouse Casz1 is orthologous to *Drosophila* Cas and confers mid/late temporal identity in RPCs, allowing the generation of rod photoreceptors and bipolar cells

[1]Cellular Neurobiology Research Unit, Institut de recherches cliniques de Montreal (IRCM), Montreal H2W 1R7, Canada. [2]Molecular Biology Program, Université de Montréal, Montreal H3T 1J4, Canada. [3]Lunenfeld-Tanenbaum Research Institute, Sinai Health System, Toronto M5G 1X5, Canada. Department of Ophthalmology and Vision Science, Department of Lab Medicine and Pathobiology, University of Toronto, Toronto M5S 1A8, Canada. [4]UCL Institute of Ophthalmology, London EC1V 9EL, UK. [5]NIHR Biomedical Research Centre at Moorfields Eye Hospital NHS Foundation Trust and UCL Institute of Ophthalmology, London EC1V 2PD, UK. [6]Department of Medicine, Université de Montréal, Montreal H3T 1J4, Canada. [7]Department of Anatomy and Cell Biology, Division of Experimental Medicine, McGill University, Montreal H4A 3J1, Canada.
*Present address: Ottawa Hospital Research Institute, Ottawa K1H 8L6, Canada. ‡Present address: National Eye Institute, Bethesda, MD 20892, USA. §Present address: Children's Medical Research Institute, University of Sydney, Sydney NSW 2145, Australia.

¶Author for correspondence (michel.cayouette@ircm.qc.ca)

P.M., 0000-0002-5708-6218; M.C., 0000-0003-4655-9048

Handling Editor: Steve Wilson
Received 23 January 2020; Accepted 19 August 2020

Development (2020) 147, dev188730. doi:10.1242/dev.188730

(Mattar et al., 2015). Intriguingly, however, Ikzf1 does not appear to regulate cone photoreceptor production, even though these cells are also produced during early stages of retinogenesis, from around E11.5 to E18.5 (Young, 1985a,b; Rapaport et al., 2004; Carter-Dawson and LaVail, 1979b; Turner et al., 1990). Considering that the *Drosophila* temporal identity cascade appears to be conserved, at least partially, to regulate temporal patterning in mammalian RPCs, we hypothesised that other homologs of the fly cascade might regulate the timely production of cone photoreceptors.

Here, we show that Pou2f1 and Pou2f2 (originally named Oct-1 and Oct-2), the mammalian homologs of *Drosophila* Nub and Pdm2, respectively, regulate the timely production of cone photoreceptors in the mouse retina. This is achieved by the direct repressive action of Pou2f2 on the rod-inducing factor Nrl, providing a rare link between temporal identity factors and downstream regulators of cell fate choice in mammalian CNS development. Importantly, we provide evidence for cross-regulatory mechanisms operating between Pou2f1 and the other temporal identity factors Ikzf1 and Casz1, reinforcing the idea that some aspects of the strategy used to control temporal progression in fly neuroblasts are conserved in mammalian neurogenesis.

RESULTS

Pou2f1 and Pou2f2 are expressed in early retinal progenitor cells, and Pou2f1 expression is maintained in mature cone photoreceptors

We first used BLAST-P to identify *Mus musculus* proteins presenting high sequence conservation with *Drosophila melanogaster* Nub/Pdm2 proteins (Altschul et al., 1990). We found that the DNA-binding POU-specific domain and POU-homeodomain of Nub/Pdm2 are highly homologous to mouse Pou2f1 and Pou2f2, respectively (Fig. S1A), as previously reported for human POU2F1 and POU2F2 (Lloyd and Sakonju, 1991). To study expression of Pou2f1 and Pou2f2 proteins in the developing retina, we first validated antibodies. As it has previously been reported that Pou2f1 is expressed in the developing retina at E11.5 (Donner et al., 2007), we asked whether antibodies against Pou2f1 and Pou2f2 recognise the appropriate band size in western blots from E12 retinal extracts. We found that the Pou2f1 antibody recognises two bands around 80 kDa, corresponding to the size of two of the isoforms of Pou2f1, whereas the Pou2f2 antibody recognises two bands at 70 kDa and 65 kDa, corresponding to the size of the two Pou2f2 isoforms (Fig. S1B). To determine whether the antibodies showed any cross-reactivity in immunostaining, we electroporated either CAG:Pou2f1-IRES-GFP or CAG:Pou2f2-IRES-GFP in P0 retinas and stained sections 48 h later. We found that the anti-Pou2f1 antibody detected overexpressed Pou2f1, but not Pou2f2, and, conversely, the anti-Pou2f2 antibody detected overexpressed Pou2f2 but not Pou2f1 (Fig. S1C-F′), indicating that each antibody does not crossreact with the other Pou2f protein. Next, we generated shRNAs and gRNAs targeting both Pou2f1 and Pou2f2, and electroporated P0 retinal explants with CAG:GFP, CAG:Pou2f1-IRES-GFP or CAG:Pou2f2-IRES-GFP along with the respective gRNA or shRNA vector (Fig. S1G, Table S1), and stained the retina 3 days later with the antibodies against Pou2f1 or Pou2f2. We found a considerable decrease in immunostaining signal in both cases (Fig. S1H-S″). Furthermore, the shRNA vectors significantly decreased the levels of Pou2f1 and Pou2f2 proteins detected by western blot after co-expression in HEK293 cells (Fig. S1T-U). Together, these results show that the Pou2f1 and Pou2f2 antibodies recognise the right antigen and at the same time validate the targeting efficiency of our gRNAs and shRNAs.

Using these validated reagents, we first studied the spatiotemporal expression pattern of Pou2f1 and Pou2f2 in the developing mouse retina. We found Pou2f1 and Pou2f2 positive (Pou2f1/2$^+$) cells of the retinal progenitor layer (RPL) that co-labelled with proliferating cell markers Ki67 or EdU from E11.5 to E15.5, indicating expression in RPCs. Starting from E15.5, however, the number of Pou2f1/2$^+$ RPCs declined (Fig. 1A-F″) and only a few RPCs expressing Pou2f1 at low levels and virtually no RPCs expressing Pou2f2 by P0 were found (Fig. S2A-B′). We observed Pou2f1/Pou2f2 co-labelling in the majority of cells at E11 (Fig. S2C), consistent with recently published RNA-seq datasets (Fig. S2D) (Clark et al., 2019; Hoshino et al., 2017; Aldiri et al., 2017). This demonstrates that Pou2f1 and Pou2f2 are expressed in mitotic RPCs during the period of cone genesis, but not in RPCs generating late-born cell types.

At E15.5, some Pou2f1$^+$ cells co-labelled with Rxrg, which labels cone photoreceptors on the apical-most region of the retina, whereas others co-labelled with Vsx2, a marker for RPCs at this stage, suggesting Pou2f1 expression in both cones and dividing RPCs (Fig. S2E). By E17.5 and onwards, Pou2f1 was expressed primarily in Rxrg$^+$, Lim1$^+$ (horizontal cell marker) and Brn3b$^+$ (ganglion cell marker) cells (Fig. 1G-L″, Fig. S2F-G″). Consistent with these data, when we analysed expression of Pou2f1 in a published RNA-seq dataset of sorted cone photoreceptors, we found high expression of Pou2f1 mRNA (Daum et al., 2017). These data suggest that Pou2f1 expression is maintained in mature cone, horizontal and ganglion cells.

The antibodies against Pou2f2 and Rxrg were both raised in rabbits, precluding double staining. We therefore used the Chrnb4-eGFP mouse line, which expresses GFP specifically in cones and ganglion cells, to assess Pou2f expression in these cells at E14.5 (Siegert et al., 2009; Decembrini et al., 2017). Some apically located cells co-labelled with Pou2f2 and GFP, and were negative for Brn3b, consistent with expression in a subset of cones, whereas other Pou2f2$^+$ cells were co-labelled with Brn3b, indicating expression in RGCs (Fig. S2H).

Next, we asked whether POU2F1 and POUF2 are also expressed in the developing human retina. Our POU2F2 antibodies did not produce a signal in human retinas. However, the POU2F1-specific antibody stained cells in the progenitor layer that lacked OTX2 and BRN3B, while others expressed OTX2 or BRN3B at foetal week (FW) 12 (Fig. 1M), suggesting expression in RPCs, RGCs and differentiating photoreceptors. From FW15 to FW19, POU2F1 labelling in the progenitor layer decreased, but was maintained in cells found at the apical side of the outer nuclear layer (ONL) in the macula region, where cones reside, and co-labelled with OTX2 (Fig. 1N), a marker of photoreceptors in this layer. Some POU2F1$^+$ cells also co-labelled with L/M-OPSIN and ONECUT2, cone and horizontal cell markers, respectively (Fig. 1M‴-Q‴). To further characterise the expression of POU2F1 in human retinal tissue, we generated human embryonic stem cell-derived retinal organoids using a previously published protocol (Gonzalez-Cordero et al., 2017). As observed in human foetal retinas, we found that POU2F1 was expressed in proliferating KI67$^+$ progenitors in early-stage organoids (Fig. S2I), whereas its expression decreased in the progenitor layer at later stages, but remained in differentiated cones at 24 weeks, as determined by co-staining with S-OPSIN, L/M-OPSIN and ARRESTIN (Fig. S2J). Thus, POU2F1 is expressed in early- but not late-stage RPCs and is maintained in mature cone photoreceptors in the human retina, similar to what we observed in the mouse retina.

Sustained Pou2f1 and Pou2f2 expression expands cone production outside the normal developmental window

As expression of Pou2f1 and Pou2f2 in RPC is lost when cone production is over, we wanted to investigate whether their sustained expression could extend the period of cone production. We

Development (2020) 147, dev188730. doi:10.1242/dev.188730

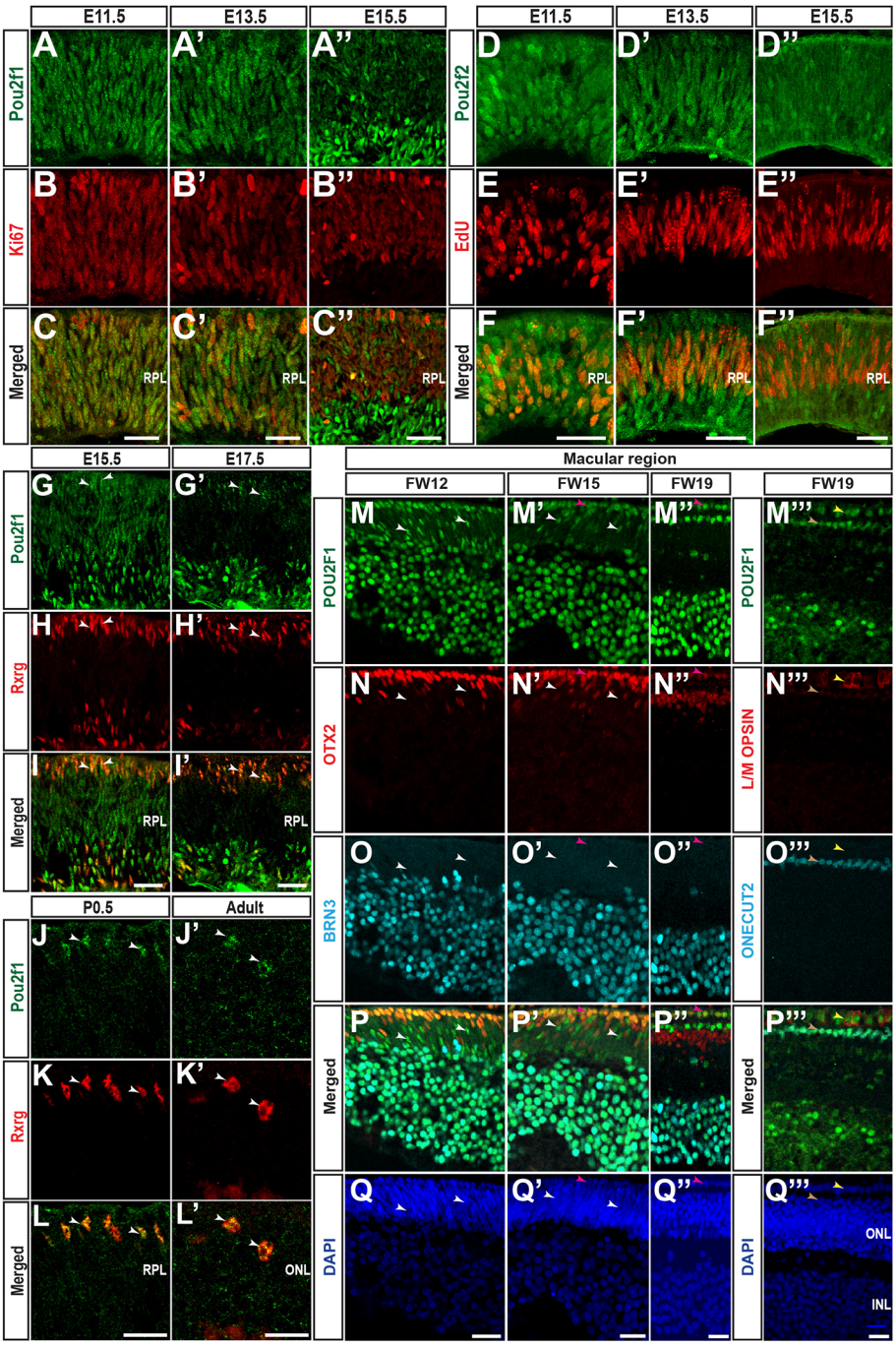

Fig. 1. Pou2f1 and Pou2f2 expression in developing mouse and human retinas. (A-F″) Co-immunostaining for Pou2f1 or Pou2f2, the proliferation marker Ki67 or EdU (injected 1 h before sacrifice) in the mouse retina at different stages, as indicated. (G-L′) Co-immunostaining for Pou2f1 (green) and the cone marker Rxrg (red) at different stages of mouse retinogenesis. Arrowheads indicate cone photoreceptors expressing Pou2f1. (M-Q‴) Co-immunostaining for POU2F1, OTX2, L/M OPSIN, BRN3, ONECUT2 and DAPI on human retinal sections at foetal weeks (FW) 12, 15, and 19. White arrowheads indicate $OTX2^{-}BRN3^{-}$ cells expressing POU2F1. Magenta arrowheads indicate $OTX2^{+}BRN3^{-}$ cells expressing POU2F1. Yellow and brown arrowheads indicate L/M $OPSIN^{+}$ and $ONECUT2^{+}$ cells, respectively, expressing POU2F1. RPL, retinal progenitor layer; ONL, outer nuclear layer; INL, inner nuclear layer. Scale bars: 20 µm in A-I′; 10 µm in J-Q‴.

electroporated CAG:GFP, CAG:Pou2f1-IRES-GFP or CAG:Pou2f2-IRES-GFP vectors in E14 retinal explants, and assessed the percentage of cones produced by co-staining with GFP and cone markers 19 days later (Fig. 2A). Interestingly, we found an increase in the proportion of GFP^{+} cells that co-expressed Rxrg and S-opsin after Pou2f1 or Pou2f2 expression (Fig. 2B-G). These additional cones might have arisen from an increased production during the normal temporal window of cone genesis or from an extension of this window into later stages. To distinguish between these possibilities, we added EdU to the culture medium 5 days after electroporation of Pou2f1 or Pou2f2, when cone production is normally over, and analysed the explants 14 days later (Fig. 2H). Although virtually no S-$opsin^{+}/EdU^{+}/GFP^{+}$ cells were detected in controls (1/455 cells counted), as expected, we found a significant fraction of these cells after Pou2f1 or Pou2f2 overexpression (Fig. 2I-M). Moreover, we did not observe an increase in the total number of EdU^{+}/GFP^{+} cells, suggesting that misexpression of Pou2f1 or Pou2f2 does not affect the proliferative potential of early RPCs (Fig. S3A). These results suggest that sustained expression of Pou2f1 and Pou2f2 in RPCs extends the period of cone production.

Ectopic expression of Pou2f1 or Pou2f2 in late-stage retinal progenitors induces cone production at the expense of late-born fates

Postnatal murine RPCs have normally lost the competence to generate cones. To determine whether Pou2f1/2 is sufficient to confer competence to generate cones in late-stage RPCs, we first infected P0 retinal explants with retroviral vectors expressing

Development (2020) 147, dev188730. doi:10.1242/dev.188730

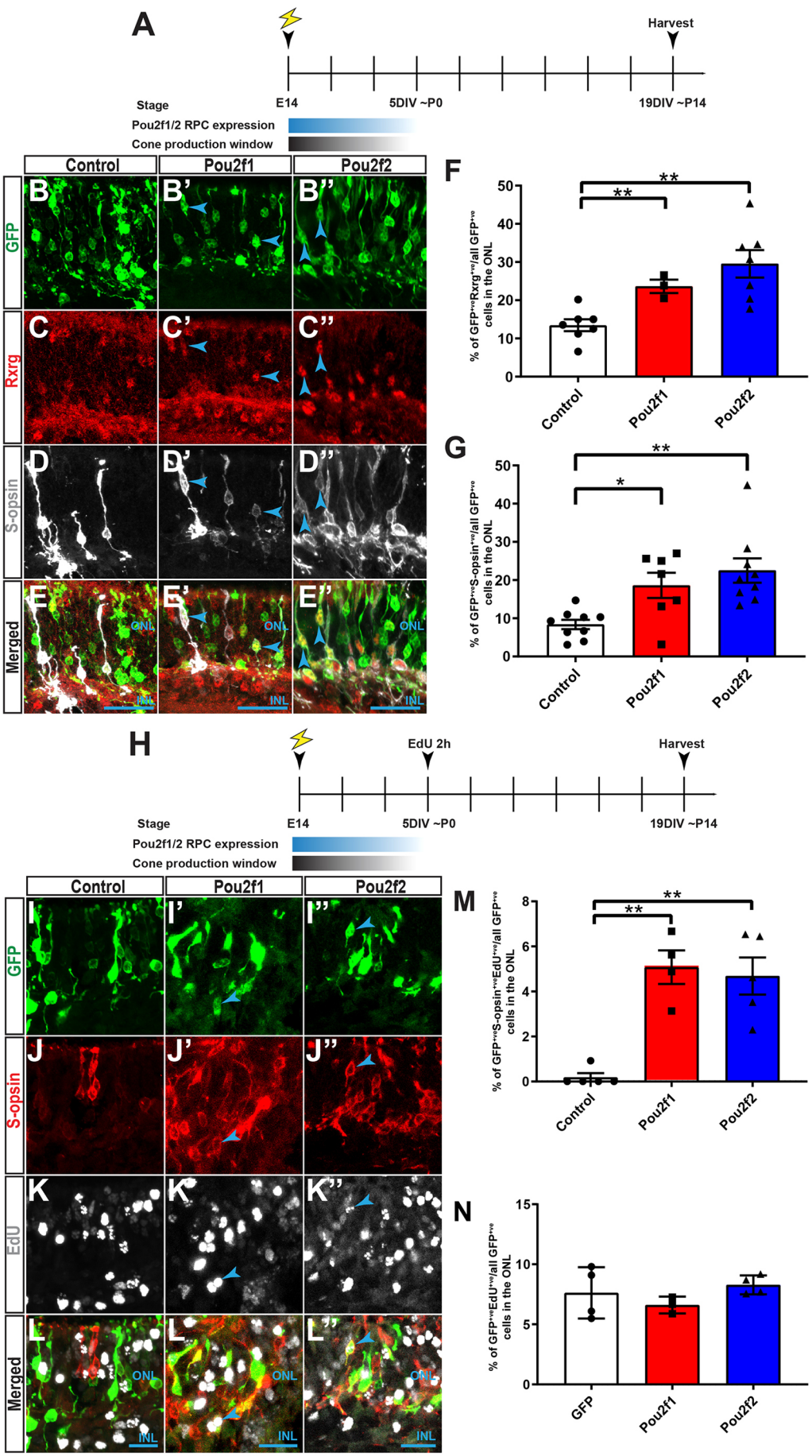

Fig. 2. Continuous Pou2f1 and Pou2f2 expression prolongs the cone production window. (A) Schematic representation of the experimental paradigm for results shown in B-G. (B-E″) *Z*-stack projection of *ex vivo* electroporated cells with a GFP control vector (B-E), Pou2f1-IRES-GFP (B′-E′) or Pou2f2-IRES-GFP (B″-E″) stained for the cone photoreceptor markers Rxrg and S-opsin. Arrowheads indicate GFP$^+$ cells expressing both Rxrg and S-opsin. (F,G) Quantification of GFP$^+$ cells expressing Rxrg (control, *n*=7; Pou2f1, *n*=3; Pou2f2, *n*=7) (F) or S-opsin (control, *n*=9; Pou2f1, *n*=7; Pou2f2, *n*=9) (G) 19 days after *ex vivo* electroporation at E14. (H) Schematic representation of the experimental paradigm for results shown in I-N. (I-L″) *Z*-stack projection of the ONL region of retinal explants electroporated with control GFP (*n*=4) (I-L), Pou2f1-IRES-GFP (*n*=3) (I′-L′) or Pou2f2-IRES-GFP (*n*=4) (I″-L″) and stained for EdU and S-opsin. Arrows indicate GFP$^+$S-opsin$^+$ cells. (M) Quantification of the number of GFP$^+$EdU$^+$ cells expressing S-opsin in each electroporated condition, as indicated. (N) Quantification of all EdU$^+$GFP$^+$ cells in explants analysed in M. **P*<0.05, ***P*<0.01 (one-way ANOVA with Dunnett's test). Data are mean±s.e.m. INL, inner nuclear layer; ONL, outer nuclear layer. Scale bars: 20 µm in B-E″; 10 µm in I-L″.

Development (2020) 147, dev188730. doi:10.1242/dev.188730

Venus, Pou2f1-IRES-Venus or Pou2f2-IRES-Venus and analysed cell type composition and clone size 14 days later (Fig. 3A). Retroviral-mediated expression of Pou2f1 at P0 increased the production of Rxrg^{+}/S-opsin^{+}, PNA^{+}/S-opsin^{+} and Rxrg^{+}/Otx2^{+} cells in the photoreceptor layer (Fig. 3B-E″, Fig. S3A-E′). Pou2f2, in contrast, induced the production of Rxrg^{+} cells located in the photoreceptor layer, but these cells did not express mature cone markers like S-opsin (Fig. 3B″-E″). As Rxrg is also expressed in ganglion cells, we wondered whether the Rxrg^{+} cells observed after Pou2f2 expression might be ganglion cells mis-localised in the photoreceptor layer. However, the Rxrg^{+} cells in the photoreceptor layer observed after expression of Pou2f2 were co-labelled with

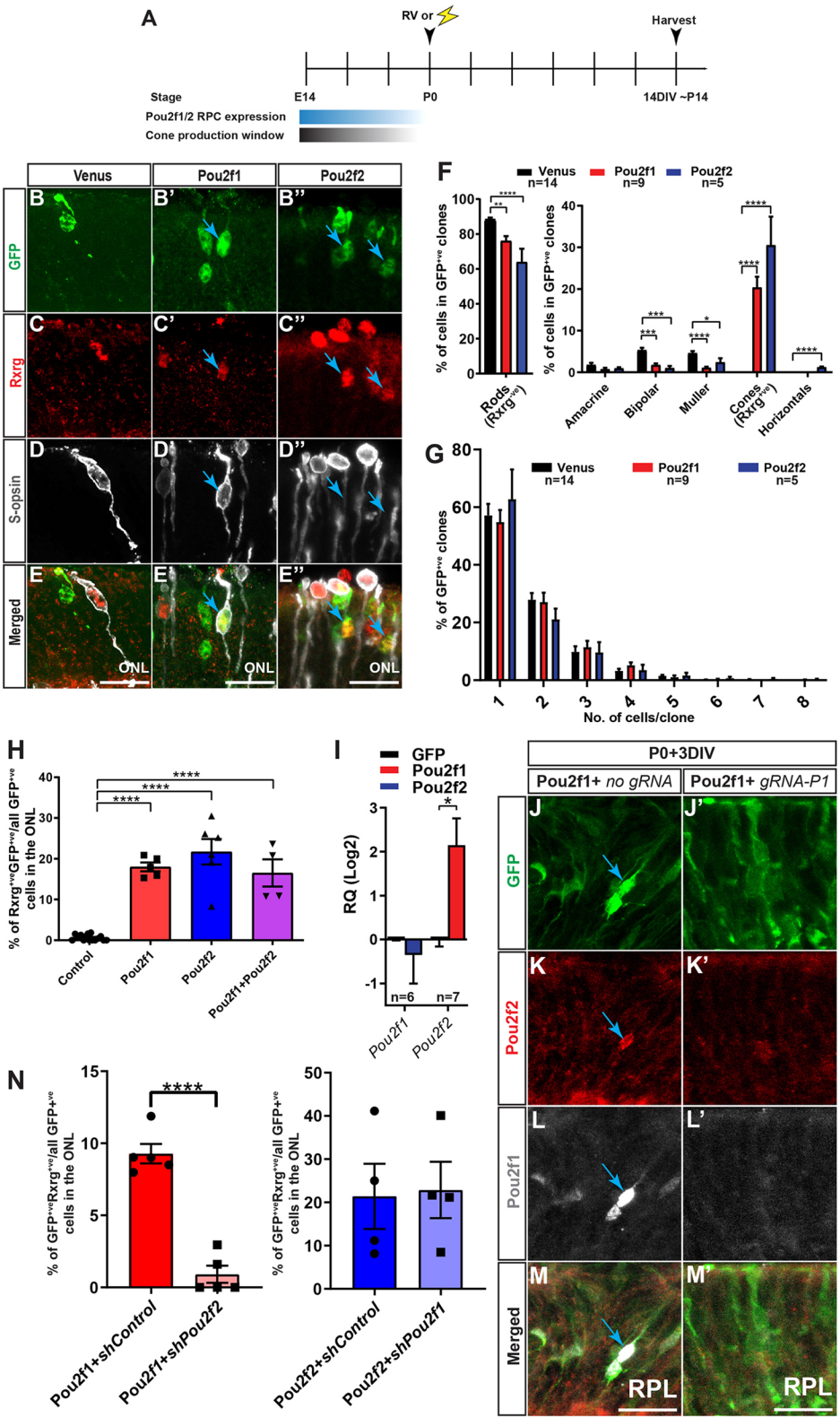

Fig. 3. Pou2f1 and Pou2f2 are sufficient to induce cone production in mid/late-stage mouse retina. (A) Schematic representation of the experimental paradigm for results shown in B-G. (B-E″) *Z*-stack projection of retrovirally infected cells with Venus control (B-E), Pou2f1-IRES-GFP (B′-E′) and Pou2f2-IRES-GFP (B″-E″) stained for Rxrg and S-opsin as cone markers. Arrows indicate GFP^{+}Rxrg^{+} cells. (F,G) Retroviral clonal analysis of control (1206 clones counted), Pou2f1 (639 clones counted) or Pou2f2 (376 clones counted) misexpression in mid-late stage retinas. *n* values are indicated in the graph. (F) Cell type analysis of GFP^{+} cells found in the clones. Clones were counted using Rxrg as a marker, whereas the other cell types were quantified based on morphology and laminar positioning in the retina. (G) Average size distribution of the clones presented in F. (H) Quantification of GFP^{+} cells expressing Rxrg in the ONL following *in vivo* electroporation of GFP (*n*=15), Pou2f1 (*n*=5), Pou2f2 (*n*=6) or Pou2f1+Pou2f2 (*n*=4). (I) RT-qPCR analysis of *Pou2f1* and *Pou2f2* expression from sorted GFP^{+} cells 9 h after electroporation at P0 in retinal explants of either control GFP, Pou2f1-IRES-GFP or Pou2f2-IRES-GFP. *n* values are indicated in the graph. (J-M′) Retinal explant electroporated at P0 with Pou2f1-IRES-GFP with no *gRNA* (J-M) or *gRNA-Pou2f1* (J′-M′), cultured for 3 DIV, and stained for Pou2f2 (K,K′) or Pou2f1 (L,L′). (N) Quantification of the number of GFP^{+}Rxrg^{+} cells after Pou2f1 misexpression with either shControl-GFP (*n*=5) or shPou2f2-GFP (*n*=5), and vice versa (Pou2f2+shControl, *n*=4; Pou2f2+shPou2f1, *n*=4) in P0 retinal explants. **P*<0.05, ***P*<0.01, ****P*<0.001, *****P*<0.0001 [one-way ANOVA with Dunnett test (F-H), Mann–Whitney test (I) or two-way ANOVA with Dunnett (G) and two-tailed unpaired *t*-test (N)]. Data are mean±s.e.m. DIV, days *in vitro*; RQ, relative quantitation; RPL, retinal progenitor layer; ONL, outer nuclear layer. Scale bars: 20 µm.

Development (2020) 147, dev188730. doi:10.1242/dev.188730

Otx2, which labels photoreceptors in this layer, and never stained for the RGC marker Brn3b (Fig. S3B″-E‴), excluding this possibility. Pou2f2 also induced the production of a small number of horizontal cells, another early-born cell type (Fig. 3F, Fig. S3F-H′). Interestingly, both Pou2f1 and Pou2f2 promoted Rxrg^{+} cells at the expense of late-born cell types (rod, bipolar and Müller), without changing the distribution of clone size (Fig. 3F,G), suggesting that Pou2f1 and Pou2f2 do not trigger cone production by altering proliferation or cell death.

We next assessed whether Pou2f1 and Pou2f2 could promote cone production *in vivo*. We electroporated mouse retinas at P0 with GFP, Pou2f1-IRES-GFP or Pou2f2-IRES-GFP. Two weeks later, the retinas were stained for GFP, Rxrg and S-opsin. Although GFP-transfected RPCs did not generate cones at this stage, as expected, misexpression of either Pou2f1 or Pou2f2 substantially increased the proportion of Rxrg^{+} cells located in the photoreceptor layer (Fig. 3H, Fig. S3I-L″). The Rxrg^{+} cells induced by Pou2f1 also expressed S-opsin, whereas those induced by Pou2f2 did not (Fig. S3I″-L″), as observed in retinal explants (see Fig. 3B-G). Interestingly, Pou2f1 misexpression did not promote M-opsin-expressing cells (data not shown). Together, these results indicate that ectopic expression of Pou2f1 in P0 RPCs is sufficient to trigger the production of S-cones, whereas Pou2f2 induces the production of immature cones.

Interestingly, co-electroporation of Pou2f1 and Pou2f2 does not elicit an additive effect in the number of cones produced by P0 RPCs (Fig. 3H), suggesting that Pou2f1/2 might function in the same genetic pathway. Consistently, we found that Pou2f1 significantly increases Pou2f2 transcript levels 9 h after electroporation, whereas Pou2f2 has no effect on Pou2f1 transcripts (Fig. 3I). Moreover, when we electroporated Pou2f1 in P0 retinal explants and stained for Pou2f2 3 days later, we found that Pou2f1 increases Pou2f2 levels in some GFP^{+} cells, whereas co-electroporating Pou2f1 with a Pou2f1 gRNA and Cas9 abrogates this effect (Fig. 3J-M′). These results suggest that Pou2f1 upregulates Pou2f2 expression. To test the functional hierarchy of the Pou2f1→Pou2f2 cascade in cone production, we co-electroporated P0 retinas with Pou2f1 while knocking-down Pou2f2 with an shRNA, or vice versa, and assessed cone production 14 days later. Whereas Pou2f1 increased cone numbers when co-expressed with a control shRNA, as predicted, it was unable to do so when Pou2f2 was knocked down (Fig. 3N). In contrast, Pou2f2 was equally able to promote cones in the presence or absence of Pou2f1 (Fig. 3N). Together, these results support a model in which Pou2f1 requires Pou2f2 to promote the cone fate.

Pou2f1 and Pou2f2 are required for cone cell fate specification in the developing retina

To determine whether Pou2f1 and Pou2f2 are required for cone production, we first knocked down their expression using shRNA and CRISPR/Cas9 gRNA in E14 retinal explants, a stage when cones are normally produced. Three weeks later, we determined the proportion of electroporated cells that became cones by counting the proportion of GFP^{+}/Rxrg^{+} cells in the photoreceptor layer. With both approaches, we found a significant decrease in the proportion of cones produced (Fig. S4A-C). Given that shRNAs were delivered using retroviral vectors, we were also able to determine the effect of Pou2f1 and Pou2f2 knockdown on other retinal fates and clone size. We found that the loss of cones is compensated for by an increase in late-born rod production after Pou2f2 knockdown, while Pou2f1 knockdown does not significantly affect other fates, most likely because the decrease in cone production is less than with Pou2f2 knockdown (Fig. S4B). Both Pou2f1 and Pou2f2 knockdown did not affect clone size distribution (Fig. S4C). Finally, Cre electroporation in Pou2f2$^{fl/fl}$ retinal explants at E13 also significantly reduced the generation of cones (Fig. S4D). These results suggest that Pou2f1 and Pou2f2 are required for cone photoreceptor development.

Next, we sought to determine whether Pou2f1 and Pou2f2 are required for cone production *in vivo*. As our data suggest that Pou2f2 lies downstream of Pou2f1 and is required for the cone-inducing activity of Pou2f1, we decided to focus our analysis on Pou2f2. As *Pou2f2*$^{-/-}$ mice die shortly after birth (Konig et al., 1995), we generated conditional knockouts (cKO) by crossing Pou2f2$^{fl/fl}$ mice (Hodson et al., 2016) with two different Cre driver lines: the alpha-Pax6-Cre line, which drives Cre expression in peripheral RPCs from E10 onwards (Marquardt et al., 2001), and the Chx10-Cre^{ERT2} line (RIKEN Bioresource Centre RRID: IMSR_RBRC06574), which allows tamoxifen-inducible activation of Cre. When we stained the peripheral retina of αPax6-Cre^{+};Pou2f2$^{fl/fl}$ (αPax6Cre-Pou2f2 cKO) with the Pou2f2 antibody, we observed a reduction in immunostaining signal specifically in Cre^{+} cells at E12 (Fig. S4E-G′) and in RGCs at P14 (Fig. S4H-J′). To assess the recombination efficiency in the Chx10-Cre^{ERT2} mice, we crossed them with Rosa26-tdT reporter mice, injected tamoxifen at E11.5, and assessed tdT expression at E13.5. As expected, we found robust recombination throughout the retina (Fig. S4K-M′). Next, we stained retinas from Chx10-Cre^{ERT2}; Pou2f2$^{fl/fl}$ (Chx10Cre-Pou2f2 cKOs) for Pou2f2 and observed a reduction in immunostaining signal in the GCL at E17.5 (Fig. S4N-P′). These results provide additional evidence for the specificity of the Pou2f2 antibody and validate both conditional knockout approaches.

Next, we stained retinal sections from P14 αPax6Cre-Pou2f2 cKO and control mice for markers of various retinal cell types. We found that deletion of Pou2f2 leads to a decrease in cone photoreceptors and horizontal cells, as determined by counting Rxrg-, PNA-, Arr3-, Cnga3- and Lim1-expressing cells (Fig. 4A-F). We did not observe any significant change in the number of amacrine (Pax6), bipolar (Chx10), ganglion (Brn3b) or Müller (Sox2) cells produced in these retinas (Fig. 4F). We also observed a decrease in Arr3 staining in flat-mounts of temporal regions of P14 cKO retinas (Fig. 4G-G″). Finally, we observed a similar decrease in cone numbers (Rxrg^{+} in the photoreceptor layer) and a compensatory increase in rod numbers (Nrl^{+} cells) in the Chx10Cre-Pou2f2 cKO retinas compared with controls at E17.5 (Fig. 4H-J). Collectively, these experiments demonstrate that Pou2f2 is required, at least partially, for the production of cone and horizontal cells in the developing retina.

Ikzf1 induces Pou2f1, which in turn represses Casz1

We next investigated whether Pou2f1/2 might be part of a temporal identity cascade controlled by cross-regulatory mechanisms, similar to that observed in *Drosophila*, where Hb activates Kr, which then activates Pdm to ensure temporal identity progression in neuroblasts (Doe, 2017). We first hypothesised that Ikzf1 might induce Pou2f1 and Pou2f2 expression in mouse RPCs, as they are expressed at the same stages. To test this idea, we transfected E14 retinal explants with vectors expressing GFP, Ikzf1-IRES-GFP or Ikzf1-VP16-IRES-GFP. After 10 h, a time point when the majority of GFP^{+} cells are still RPCs, we sorted the GFP^{+} cells and isolated total RNA for RT-qPCR (Fig. 5A). We found that Ikzf1 and Ikzf1-VP16 induced or repressed Pou2f1/2, respectively (Fig. 5B,C). Interestingly, we found that Ikzf1 has no effect on Pou2f1 expression in P0 retinal explants (Fig. 5D,E), suggesting that Ikzf1 promotes Pou2f1 expression in early but not late RPCs.

In a previous study, we reported that Ikzf1 represses Casz1 expression, likely via an indirect mechanism (Mattar et al., 2015).

Development (2020) 147, dev188730. doi:10.1242/dev.188730

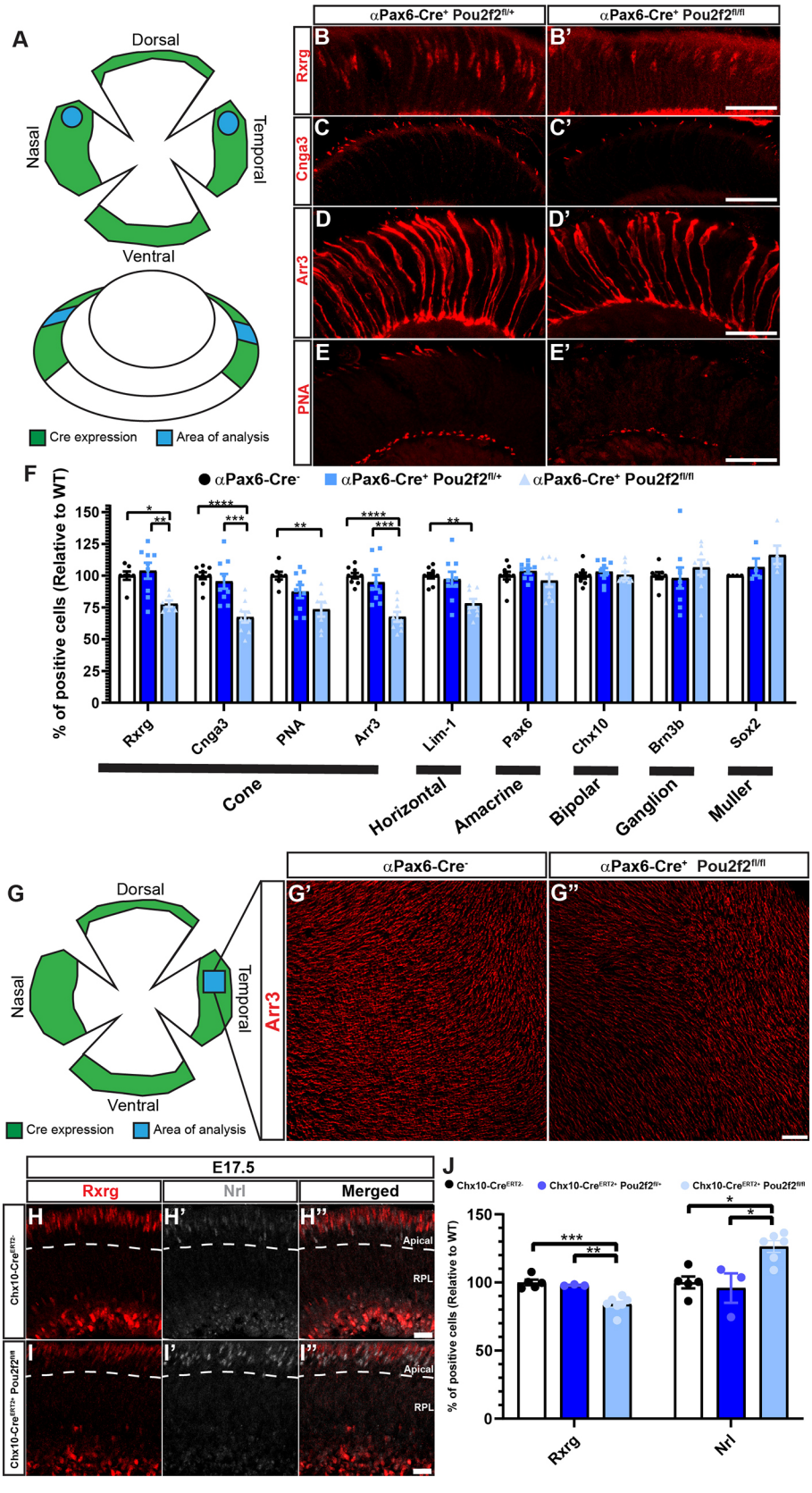

Fig. 4. Pou2f2 is required for cone development in the developing mouse retina. (A) Diagram showing area of analysis. (B-E′) Immunostaining for Rxrg (B,B′), Cnga3 (C,C′), Arr3 (D,D′) and PNA (E,E′) in either αPax6-Cre^{+} Pou2f2$^{fl/+}$ (B-E) or αPax6-Cre^{+} Pou2f2$^{fl/fl}$ (B′-E′) mouse retinas at P14. (F) Quantification of retinal cell types using various markers [αPax6-Cre^{+}: Cnga3, Arr3, Lim1, Pax6 and Chx10 (n=9); Brn3b (n=8); Rxrg and PNA (n=7); Sox2 (n=4); αPax6-Cre^{+} Pou2f2$^{fl/+}$: Cnga3, Arr3, Lim1, Pax6, Chx10, Brn3b, Rxrg and PNA (n=9); Sox2 (n=4); αPax6-Cre^{+} Pou2f2$^{fl/fl}$: Cnga3, Arr3, Lim1, Pax6, Chx10 and Brn3b (n=9); Rxrg and PNA (n=7); Sox2 (n=5)]. (G-G″) Flat-mount area of analysis and flat-mount image of P14 retinas of either αPax6-Cre^{-} (G′) or αPax6-Cre^{+} Pou2f2$^{fl/fl}$ (G″). (H-I″) Immunostaining for Rxrg (H,I) or Nrl (H′,I′) in either Chx10-Cre^{ERT2-} (H,H′) or Chx10-Cre^{ERT2+} Pou2f2$^{fl/fl}$ (I,I′) mouse retinas at E17.5. (J) Quantification of the percentage of Rxrg^{+} (Chx10-Cre^{ERT2-}, n=5; Chx10-Cre^{ERT2+} Pou2f2$^{fl/+}$, n=3; Chx10-Cre^{ERT2+} Pou2f2$^{fl/fl}$, n=7) and Nrl^{+} (Chx10-Cre^{ERT2-}, n=5; Chx10-Cre^{ERT2+} Pou2f2$^{fl/+}$, n=3; Chx10-Cre^{ERT2+} Pou2f2$^{fl/fl}$, n=6) cells relative to the wild type. *P<0.05, **P<0.01, ***P<0.001, ****P<0.0001 [one-way ANOVA with Tukey's test (E,J)]. Data are mean±s.e.m. Scale bars: 20 µm in B-E′; 100 µm in G′-G″; 10 µm in H-I″.

Therefore, we hypothesised that Pou2f1 might function as an intermediate factor downstream of Ikzf1 to repress Casz1. Consistently, we found that ectopic Pou2f1 expression at P0, during the window of Casz1 expression, decreases the levels of *Casz1* transcripts (Fig. 5F-G). In contrast, Pou2f2 did not significantly alter expression of Casz1. Together, these results suggest that Pou2f1 is part of a cross-regulatory temporal identity cascade together with Ikzf1 and Casz1.

Development (2020) 147, dev188730. doi:10.1242/dev.188730

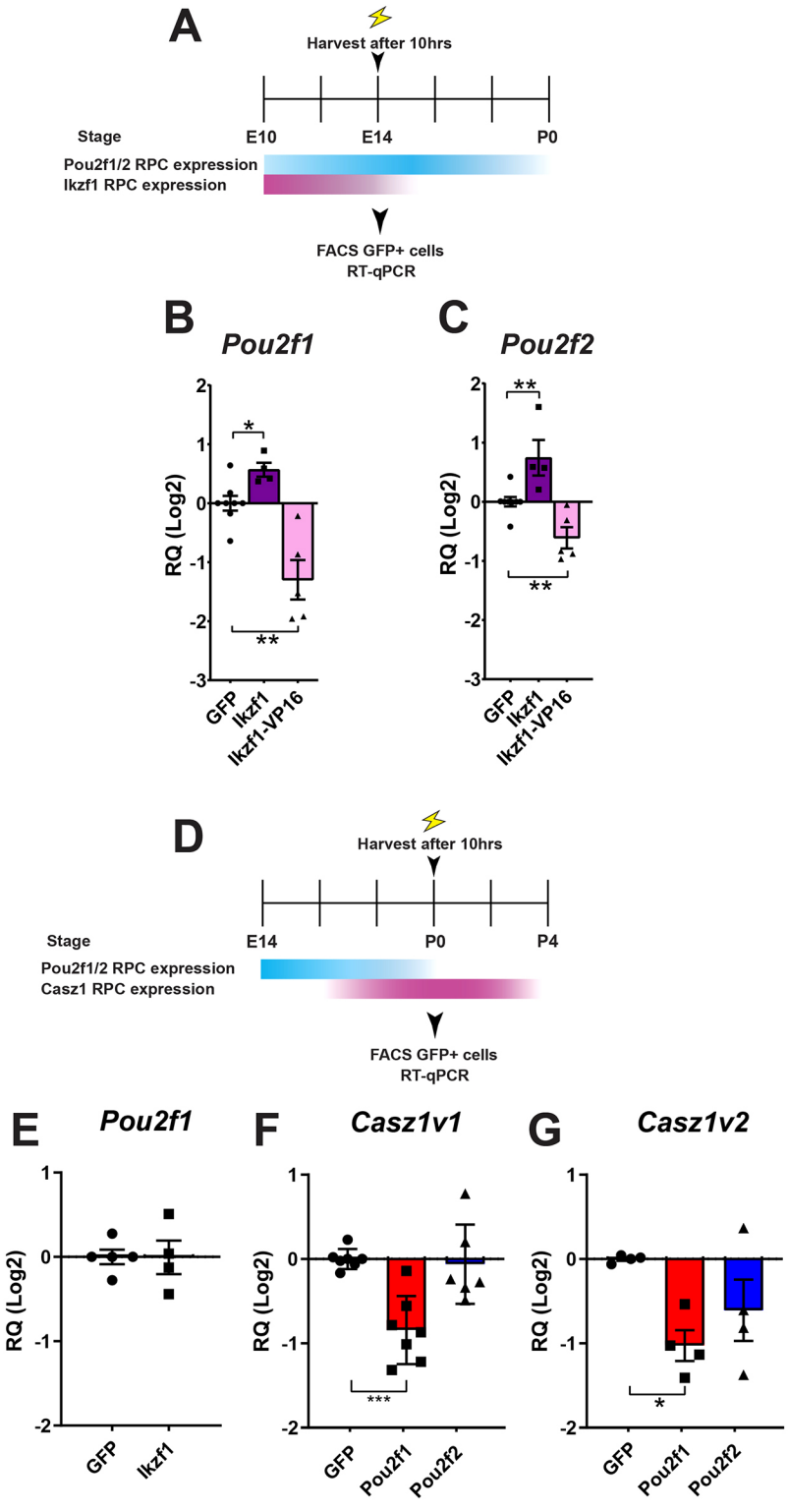

Fig. 5. Ikzf1 induces Pou2f1 expression, and Pou2f1 represses Casz1. (A) Schematic representation of the experimental paradigm for results shown in B and C. (B,C) RT-qPCR analysis of *Pou2f1* and *Pou2f2* from GFP$^+$ sorted cells after electroporation at E14 of either control GFP (*Pou2f1*, *n*=8; *Pou2f2*, *n*=8), Ikzf1-IRES-GFP (*Pou2f1*, *n*=4; *Pou2f2*, *n*=4) or Ikzf1:VP16-IRES-GFP (*Pou2f1*, *n*=5; *Pou2f2*, *n*=5). (D) Schematic representation of the experimental paradigm for results shown in E-G. (E) RT-qPCR analysis of *Pou2f1* from GFP$^+$ sorted cells after electroporation at P0 of either control GFP (*n*=5) or Ikzf1-IRES-GFP (*n*=4). (F,G) RT-qPCR analysis of the two isoforms of Casz1 (Casz1v1 and Casz1v2) after electroporation of either control GFP (*Casz1v1*, *n*=7; Casz1v2, *n*=4), Pou2f1-IRES-GFP (*Casz1v1*, *n*=7; Casz1v2, *n*=4) or Pou2f2-IRES-GFP (*Casz1v1*, *n*=6; Casz1v2, *n*=4) at P0. **P*<0.05, ***P*<0.01, ****P*<0.001 (Mann–Whitney test). Data are mean±s.e.m. RQ, relative quantitation.

Pou2f2 binds to the Nrl promoter and represses its activity

How could Pou2f1 and Pou2f2 induce the cone photoreceptor cell fate? In Olig2$^+$ early RPCs, Onecut1 and Otx2 bind to a cis-regulatory module (CRM) of the Thrb gene (active in dividing RPCs) and promote cone and horizontal cell production (Emerson et al., 2013). This CRM was cloned from the chick genome, but it remains unclear whether an equivalent CRM exists in the mouse. As this CRM is located at the downstream promoter of the chick Thrb gene, we cloned the equivalent mouse region (Thrb-PR2::GFP) as well as the upstream promoter sequence of the mouse Thrb gene (Thrb-PR1::GFP) (Fig. S5A). When we electroporated GFP constructs driven by these CRMs in E13 retinal explants, we found that they are active in cones, similar to what was observed with the chick sequences (Fig. S5B,C) (Emerson et al., 2013). To test whether Pou2f1 or Pou2f2 might regulate any of the Thrb CRMs, we co-electroporated P0 retinal explants with CAG:

Development (2020) 147, dev188730. doi:10.1242/dev.188730

mCherry to label all electroporated cells and an empty CAG vector, CAG:Pou2f1, or CAG:Pou2f2, and either ThrbPR1:GFP or ThrbPR2:GFP, and analysed GFP expression 24 h later (Fig. S5D-I). Interestingly, we found that Pou2f1 and Pou2f2 induce ThrbPR1:GFP activity but not ThrbPR2:GFP. Moreover, ThrbPR1:GFP is active as soon as mCherry expression switches on, and the GFP expression disappears 72 h after electroporation, suggesting transient activity of the CRM in the electroporated cells (data not shown). These data suggest that Pou2f1 and Pou2f2 operate in parallel with Onecut1, acting transiently at a distinct CRM of Thrb to promote the cone fate. Another role for Thrb2 has been shown at later stages during cone differentiation to promote the M-cone subtype (Ng et al., 2001; Applebury et al., 2007; Ng et al., 2009). Therefore, we tested whether Pou2f1 and Pou2f2 could promote *Thrb2* mRNA expression in a stage-dependent manner. We electroporated P0 retinal explants with CAG:GFP, CAG:Pou2f1-IRES-GFP or CAG:Pou2f2-IRES-GFP, sorted the GFP^+ cells 6 or 14 days later and assessed *Thrb2* mRNA levels. Consistent with the promoter assays described above, we found that both Pou2f1 and Pou2f2 increased *Thrb2* expression at 6 days (Fig. S5J). In contrast, both Pou2f1 and Pou2f2 had no effect on Thrb levels at 14 days. On the other hand, when we assessed *Thrb2* mRNA levels in adult αPax6-Cre Pou2f2 cKOs, we observed no change in expression, suggesting that Pou2f2 is sufficient but not required for Thrb2 expression (Fig. S5K). Finally, although POU-binding motifs were present in this CRM of Thrb, when we conducted chromatin immunoprecipitation (ChIP) in E14 mouse retinas to assess binding of Pou2f2 at this region, we did not observe significant enrichment (Fig. S5L,M). These results suggest that Pou2f1 and Pou2f2 transiently regulate Thrb2 levels to promote cone specification, but likely via an indirect mechanism.

An additional pathway known to regulate the rod to cone fate decision involves the transcription factor Nrl, which activates the nuclear receptor Nr2e3 in photoreceptor precursors to promote rod photoreceptor gene expression (Oh et al., 2008; Mears et al., 2001). In Nrl KO mice, rods are not produced and all photoreceptor precursors turn into S-cone-like cells (Mears et al., 2001). These results suggest a model in which downregulation of Nrl is important for the generation of cones, but direct repressors of Nrl remain unknown. Interestingly, we noticed that the Nrl promoter region, which has been previously characterised (Kautzmann et al., 2011), contains a POU-binding motif. Combined with our observation that Chx10Cre-Pou2f2 cKO had more Nrl^+ cells (Fig. 4J), this prompted us to postulate that Pou2f1 and Pou2f2 might repress Nrl expression. To test this hypothesis, we transfected P0 retinal explants with either GFP, Pou2f1-IRES-GFP or Pou2f2-IRES-GFP, sorted the GFP^+ cells 20 h later and analysed transcript levels by RT-qPCR. Remarkably, we found that Pou2f2 significantly reduces the levels of *Nrl* and *Nr2e3*, whereas Pou2f1 had no effect (Fig. 6A), most likely because 20 h is not long enough for Pou2f1 to trigger sufficient Pou2f2 expression to detect changes in Nrl and Nr2e3 expression. Consistent with this idea, Pou2f1 decreased Nrl transcript 6 days after transfection (Fig. 6B). Pou2f2 overexpression also reduced the number of cells staining for Nrl in the photoreceptor layer (Fig. 6C-E), supporting the RT-qPCR data. These results suggest that Pou2f2 functions as a negative regulator of Nrl.

We thus sought to determine whether Pou2f2 could repress the Nrl promoter. To do this, we co-electroporated GFP, Pou2f1-IRES-GFP or Pou2f2-IRES-GFP, together with an pNrl:dsRed reporter construct (Akimoto et al., 2006; Matsuda and Cepko, 2007) in retinal explants and studied dsRed expression 2 days later (Fig. 6F). As expected, the pNrl:dsRed reporter was robustly activated when co-electroporated with the control construct, but not when co-electroporated with Pou2f1 or Pou2f2 (Fig. 6G-I″). Importantly, when we mutated the POU-specific binding motif in the pNrl:dsRed reporter, Pou2f1 and Pou2f2 no longer repressed dsRed expression (Fig. 6J-L″). Given that Pou2f1 was unable to reduce Nrl transcripts 20 h after expression (Fig. 6B), we hypothesised that its repressive action on the Nrl promoter activity was likely mediated via upregulation of Pou2f2. If this were the case, we predicted that Pou2f2, but not Pou2f1, would bind the Nrl promoter. Consistently, ChIP-qPCR from E14 retinas detected significant enrichment of Pou2f2 at the POU-specific binding region of the Nrl promoter, whereas it was not detected in a control intronic region (Fig. 6M,N). In contrast, we failed to detect any enrichment at the same region after Pou2f1 ChIP (Fig. 6M,N). These results indicate that Pou2f2 represses Nrl expression by binding the POU motif in the Nrl promoter.

Pou2f2 functions in postmitotic photoreceptor precursors to promote the cone fate

We next wanted to determine whether Pou2f2 functions in RPCs or in postmitotic photoreceptor precursors to induce the cone fate. To address this issue, we used the wild-type and mutated Nrl promoter (mpNrl) to drive expression of Pou2f1 or Pou2f2 in photoreceptor precursors (Fig. 6O). We first validated these vectors by co-electroporating them with GFP in retinal explants at P0 and staining for Pou2f1 and Pou2f2 3 and 14 days later. We found that Pou2f1 and Pou2f2 were weakly expressed from the wild-type Nrl promoter (Fig. S6A-G″), most likely due to the negative feedback of Pou2f2 on the promoter, whereas they were robustly expressed when using mpNrl (Fig. S6H-N″).

We next stained the explants for Rxrg to assess whether overexpressing Pou2f1 or Pou2f2 in post-mitotic photoreceptor precursors was sufficient to drive cone production. Whereas mpNrl:Pou2f2 induced $Rxrg^+$ cells in the photoreceptor layer, mpNrl:Pou2f1 was much less efficient at doing so (Fig. 6P-S). As control, we found that the wild-type pNrl:Pou2f1 and pNrl:Pou2f2 did not yield any $Rxrg^+$ cells (Fig. S6F-F″). We speculate that the weak activity of the mpNrl:Pou2f1 construct on cone production is due to activation of Pou2f2 (Fig. 3G). These results indicate that expression of Pou2f2 in post-mitotic photoreceptor precursors is sufficient to promote the cone fate.

DISCUSSION

There has been considerable work carried out to understand how neural progenitor cells generate neuronal diversity in the developing central nervous system. However, not much is known about how temporal identity is encoded in progenitors to initiate the correct transcriptional code producing the appropriate cell types for a given developmental stage. In this study, we provide evidence that Pou2f1 endows RPCs with the competence to generate cone photoreceptors by promoting expression of Pou2f2, which then represses Nrl to favour the cone fate. We also provide evidence that Pou2f1 lies in a temporal cascade reminiscent of that observed in *Drosophila* neuroblasts. Ikzf1 contributes to Pou2f1 upregulation, which in turn represses the late-stage temporal factor Casz1, thereby ensuring that RPCs do not switch prematurely to a late temporal identity and allowing production of cones within the early developmental window (Fig. 7).

Encoding temporal identity versus promoting cone fate

Multiple lines of evidence support a model in which Pou2f1 confers RPCs competence to generate cones during early retinogenesis,

Development (2020) 147, dev188730. doi:10.1242/dev.188730

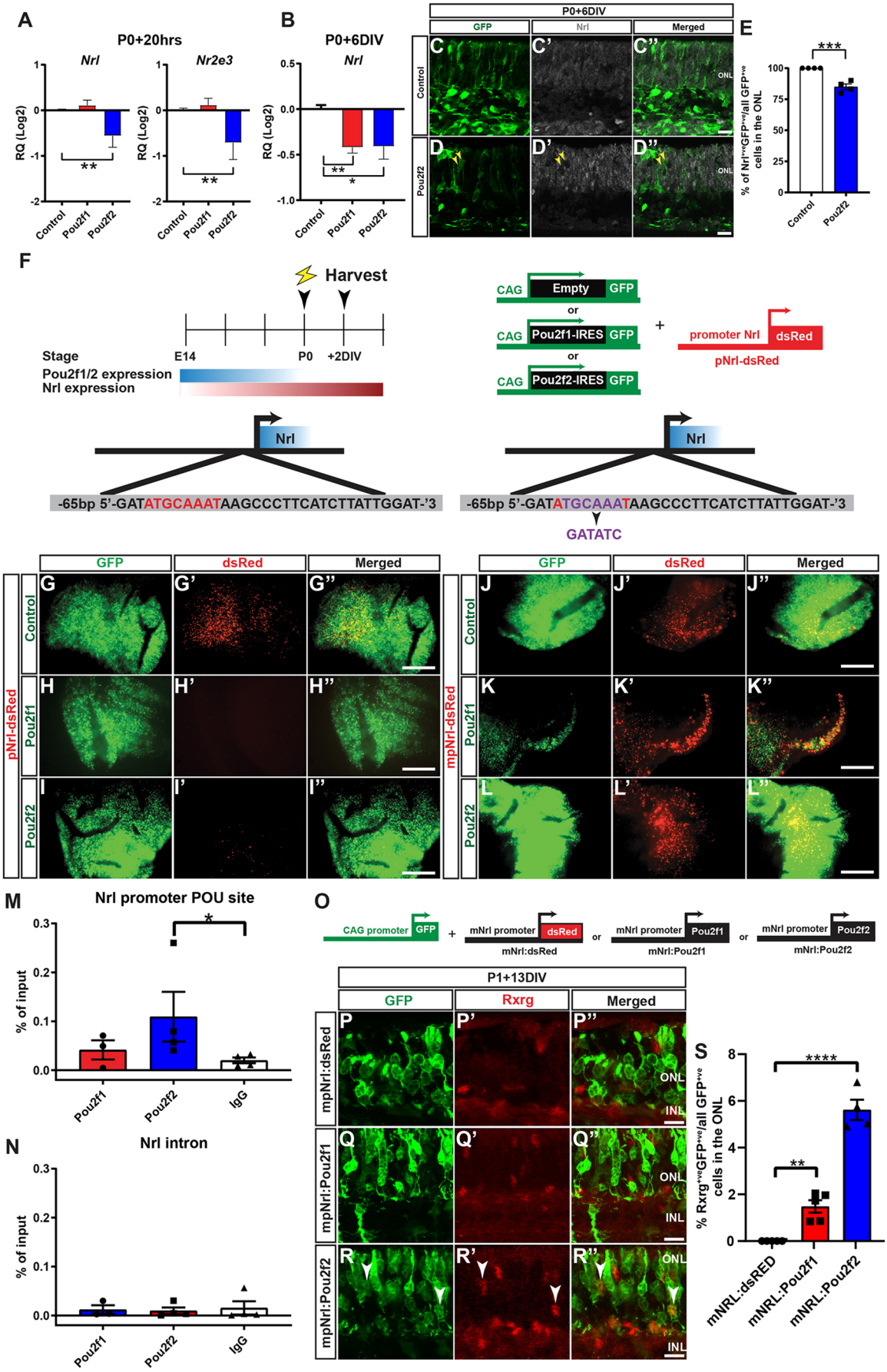

Fig. 6. See next page for legend.

Development (2020) 147, dev188730. doi:10.1242/dev.188730

Fig. 6. Pou2f2 binds to the promoter of Nrl and negatively regulates its expression. (A) RT-qPCR analysis of *Nrl* and *Nr2e3* mRNA expression following electroporation of control GFP (*n*=6), Pou2f1-IRES-GFP (*n*=6) or Pou2f2-IRES-GFP (*n*=6). (B) RT-qPCR analysis of *Nrl* from GFP$^+$ sorted cells 6 days after electroporation at P0 of either control GFP, Pou2f1-IRES-GFP or Pou2f2-IRES-GFP (*n*=5). (C-D″) Images of P0 retinal explants electroporated with either control GFP (C-C″) or Pou2f2-IRES-GFP (D-D″) and immunostained for Nrl. Yellow arrowheads show GFP$^+$ cells lacking Nrl. (E) Quantification of GFP$^+$Nrl$^+$ cells and GFP$^+$Rxrg$^+$Nrl$^-$ cells in the ONL (*n*=4). (F) Schematic representation of the experiments shown in G-L″. Retinal explants were co-electroporated with vectors expressing GFP alone, Pou2f1-IRES-GFP or Pou2f2-IRES-GFP with either control pNrl:dsRed or POU-motif mutated pNrl:dsRed (mpNrl:dsRed). (G-L″) Photomicrographs of retinal flatmounts showing reduced dsRed signal after expression of Pou2f1 (H′) or Pou2f2 (I′). (J-L″) Photomicrographs of retinal flatmounts showing loss of repression of Nrl promoter activity when Pou2f1 (K′) or Pou2f2 (L′) are co-electroporated with the mpNrl-dsRed. (M,N) Chromatin immunoprecipitation (ChIP) of Pou2f1 (*n*=3), Pou2f2 (*n*=4) or control IgG (*n*=4) followed by quantitative PCR (qPCR) for the *Nrl* promoter region containing the POU-binding site, compared with an intronic control region. (O) Schematic representation of the experimental paradigm for results shown in P-R. (P-R″) Retinal explants electroporated at P1 with either mpNrl-dsRed (P-P″), mpNrl-Pou2f1 (Q-Q″) or mpNrl-Pou2f2 (R-R″) along with CAG:GFP, cultured for 13 DIV and immunostained for Rxrg to quantify cones in the ONL. (S) Quantification of GFP$^+$ cells expressing Rxrg in the ONL (pNrl-dsRed; *n*=5; pNrl-Pou2f1, *n*=5; pNrl-Pou2f2, *n*=4). **P*<0.05, ***P*<0.01, ****P*<0.001, *****P*<0.0001 [Mann–Whitney test (A,B,M,N), two-tailed unpaired *t*-test (E), one-way ANOVA with Dunnett test (S)]. Data are mean±s.e.m. ONL, outer nuclear layer; INL, inner nuclear layer; RQ, relative quantitation. Scale bars: 10 µm in C-D″,P-R″; 50 µm in G-L″.

whereas Pou2f2 functions primarily as a classical cone fate determinant in photoreceptor precursors. First, although normal P0 RPCs are unable to generate cones, Pou2f1 is sufficient to drive production of mature cones in this context, whereas Pou2f2 is not. Thus, Pou2f1 appears able to fully open the temporal identity window in RPCs to generate cones. Subsequently, once the window of cone development is open, Pou2f2 can repress Nrl and promote cone photoreceptor specification. Consistently, expression of Pou2f1 using the Nrl promoter fails to induce a high number of cones, whereas mpNrl-Pou2f2 efficiently induces cones. Second, while the early temporal identity factor Ikzf1 induces expression of Pou2f1 followed by Pou2f2, only Pou2f1 regulates the expression of the mid/late-stage temporal factor Casz1, although we did not assess the recently discovered temporal identity factor Foxn4 (Liu et al., 2020). Thus, Pou2f1 appears to be integrated into the temporal cascade, but not Pou2f2. Whether Ikzf1 regulates Pou2f1 and Pou2f2 directly will need further investigation, but genomic regions upstream of the transcriptional start site of Pou2f1 and Pou2f2 contain multiple Ikzf 'GGGAA' consensus sequence, suggesting possible binding. Third, Pou2f2 directly binds and represses the rod determinant Nrl, which is restricted to post-mitotic photoreceptor precursors (Oh et al., 2007; Mears et al., 2001). Together with our finding that Pou2f2 is able to induce the cone fate when expressed from the Nrl promoter, this is further evidence that Pou2f2 primarily regulates cell fate decisions in postmitotic precursor cells, rather than acting in RPCs to control temporal identity. Importantly, however, we cannot rule out an additional role for Pou2f2 in dividing RPCs. Indeed, we show that Pou2f2 is expressed in early RPCs, and its overexpression not only promotes cone production, but also horizontal cells, which is consistent with a role in RPCs.

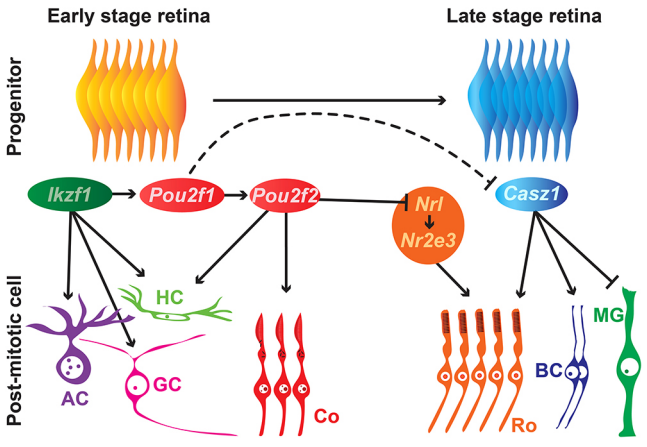

Fig. 7. Model of temporal control of cone production during retinal development. In RPCs, Ikzf1 sets up the early temporal window for horizontal, amacrine and ganglion cell production, and upregulates Pou2f1 expression, which in turn sets up the temporal window for cone production by preventing expression of the mid/late temporal factor Casz1. Pou2f1 initiates expression of Pou2f2, which binds and represses *Nrl* expression and promotes the cone fate.

Integrating Pou2f1 and Pou2f2 in the current view of cone genesis

There are currently two non-mutually exclusive pathways by which cone photoreceptors are thought to be generated. In one model, postmitotic photoreceptor precursors default to the cone fate, unless Nrl is induced, which in turn activates Nr2e3 to promote the rod fate (Oh et al., 2008; Mears et al., 2001). In another model, RPCs expressing Olig2 are pre-programmed to generate cones or horizontal cells at their last division (Hafler et al., 2012; Emerson et al., 2013). How do Pou2f1 ad Pou2f2 fit into these models?

As Pou2f1 and Pou2f2 are co-expressed in RPCs, we posit that Pou2f1 induces Pou2f2 expression prior to cell cycle exit, which may lead to sufficient levels of Pou2f2 expression in postmitotic precursors to repress Nrl. Such transient and possibly weak expression might have been difficult to detect by scRNA-seq (Clark et al., 2019). Clearly, however, Pou2f2 is also expressed in RPCs, as shown by the widespread immunostaining observed at E11.5 and as reported in scRNA-seq data (Fig. 1D-F) (Clark et al., 2019). As mentioned above, whether Pou2f2 is functionally relevant in RPCs will need further investigation, but it may have a role in controlling Olig2 progenitor fate decisions. RNA-seq analysis of Onecut1 and Onecut2 double knockout retina reveals a twofold increase in Pou2f2 mRNA levels at E14 (Sapkota et al., 2014), suggesting that Onecut1 and Onecut2 might negatively regulate Pou2f2 expression. Similar observations were recently made in the developing spinal cord, where Onecut factors, although not required for the production of V2 interneurons, repress Pou2f2 to regulate the distribution of V2 interneurons (Harris et al., 2019). A possibility is that Pou2f2 and Onecut1 and Onecut2 constitute two complementary branches of cone development. Pou2f1 might compete with Onecut1 and Onecut2 for the activation or repression of Pou2f2, respectively, in Olig2$^+$ RPCs. When Pou2f1 activity is dominant, Pou2f2 would be upregulated and progenitors would take on the horizontal fate via unknown targets of Pou2f2 and the cone fate via repression of Nrl in postmitotic photoreceptor precursors. In contrast, when Onecut1 activity is dominant, Pou2f2 would be repressed, leading cells into the Onecut1 pathway to produce cones or horizontal cells. This model could explain why inactivation of Pou2f2 (this study) or Onecut1 and Onecut2 (Sapkota et al., 2014) only reduces cone production by about 25%. Consistent with this idea, out of the two CRMs of Thrb that are active in cones, Pou2f2 activates one of the elements and Onecut1 activates the other (Fig. S6D-F) (Emerson et al., 2013). As Pou2f2, Onecut1 and

Development (2020) 147, dev188730. doi:10.1242/dev.188730

Onecut2 could potentially regulate different CRMs of Thrb, it will be interesting to assess whether Pou2f2 might also regulate Onecut1 and Onecut2 expression in Olig2^{+} RPCs.

Pou2f1/2 as negative regulators of Nrl

A long-standing question in the field has been how exactly Nrl expression is repressed in some photoreceptor precursors. Positive regulators of Nrl, such as Crx, Otx2 and RORβ have been identified (Montana et al., 2011), but negative regulators have remained elusive. Montana et al. hypothesised that a 'repressor X' could downregulate Nrl in photoreceptor precursors, to restrict expression to rod precursors. Although Onecut1 acts genetically upstream of Nrl and eventually leads to its downregulation, this effect is likely indirect (Emerson et al., 2013). While multiple studies have analysed the regulatory regions of Nrl to uncover a direct repressor (Kautzmann et al., 2011; Montana et al., 2011; Zelinger et al., 2017), the identity of such repressors remained elusive. Our work now identifies Pou2f2 as one of the direct repressors of Nrl in the developing mammalian retina. We provide evidence that Pou2f2 functions by binding a POU-binding motif located 55 bp upstream of the transcription start site of Nrl.

A potential role for Pou2f1 and Pou2f2 as temporal identity factors outside the retina

The functional role of Pou2f1 and Pou2f2 has been extensively characterised in the immune system and embryonic stem cells, but the role of Pou2f1 and Pou2f2 in the developing CNS is poorly studied. However, Pou2f1 and Pou2f2 are highly expressed in different regions of the CNS (Luchina et al., 2003; Schonemann et al., 1998; He et al., 1989; Treacy and Rosenfeld, 1992). One study found that Pou2f1 is required for the development of radial glia in *Xenopus* hindbrain and is modulated by Notch signalling (Kiyota et al., 2008). Whether Pou2f1 regulates radial glia development in mammals remains to be investigated, but the results reported here support this possibility. On the other hand, Pou2f2 is expressed in the diencephalon, mesencephalon and rhombencephalon during embryogenesis, as well as in the suprachiasmatic and medial mammillary nuclei in the adult hypothalamus (Treacy and Rosenfeld, 1992). As the global Pou2f2 mutants die at birth, it will be interesting to specifically delete Pou2f2 in these regions to assess a potential role in neurogenesis (Konig et al., 1995). Finally, as there is a high overlap of expression between Pou2f1 and Pou2f2 in the developing CNS (He et al., 1989; Treacy and Rosenfeld, 1992), it is possible that the same Pou2f1/Pou2f2 cascade operates in the specification of the neurons in other parts of the CNS.

Conclusions

Understanding how the cone photoreceptor cell fate is specified is crucial to the development of cell replacement therapies for various retinal degenerative diseases. In this study, we add to the general knowledge of cone specification mechanisms by identifying Pou2f1 and Pou2f2 as previously unknown players in cone development. Our data also help to elucidate how Nrl expression is negatively regulated during retinal development to ensure the correct balance of rod and cone production.

MATERIALS AND METHODS

Animals

All experiments in this study were done in accordance with the Canadian Council on Animal guidelines and United Kingdom Animals (Scientific Procedure) Act of 1986 and Policies on the Use of Animals and Humans in Neuroscience Research guidelines. Pregnant Pou2f2$^{fl/fl}$ females raised in the C57BL/6J background (*Mus musculus*) were sacrificed at E13.5 and retinas from embryos were extracted for pCAG:Cre electroporation and *ex vivo* retinal explant culture. αPax6-Cre^{+} Pou2f2$^{fl/fl}$ mice were at P14 at the time of cell count analysis. The Chx10-Cre^{ERT2} mouse line was generated in Dr Takahisa Furukawa's lab (Osaka University) and provided by the RIKEN BRC through the National Bio-Resource Project of the MEXT/AMED, Japan (RIKEN Bioresource RRID: IMSR_RBRC06574). Chx10-Cre^{ERT2+} Pou2f2$^{fl/fl}$ pregnant females were injected with tamoxifen at E11.5 and sacrificed at E17.5 for cell count analysis. Chx10-Cre^{ERT2+} Rosa^{tdTomato} were injected with tamoxifen at E11.5 and sacrificed at E13.5. All other mouse experiments in this study were carried out on wild-type CD1 mice (*Mus musculus*, Charles Rivers).

Tissue collection and immunofluorescence

Mouse embryos were collected from timed pregnant females with the day of vaginal plug considered as 0.5 day (E0.5). Embryos were collected from the pregnant females at E11.5, E13.5, E15.5 and E17.5, whereas eyes were collected at P0.5 and adult stages. The decapitated heads from embryos and eyes from postnatal pups were fixed for 15 min or 5 min, respectively, in 4% PFA/PBS followed by immersion in 20% sucrose/PBS for 2 h. Eyes were then embedded in OCT, frozen in liquid nitrogen and sectioned at 25 µm using a cryostat.

For immunofluorescence, retinal sections were blocked and permeabilised with the blocking solution (3% BSA in 1× PBS with 0.5% Triton X-100) for 1 h. Primary antibodies diluted in blocking solution were then applied on the sections overnight at room temperature. Sections were then washed three times for 5 min with PBS and incubated with the appropriate secondary antibodies diluted in PBS (Invitrogen, 1:1000) for 1 h at room temperature. After three 5 min PBS wash, sections were incubated in Hoechst/PBS (Invitrogen, 33342, 1:20,000) for 5 min at room temperature. Slides were washed once in PBS for 5 min and cover-slipped with Mowiol (Calbiochem). List of primary antibodies can be found in Table S2.

Retroviral constructs preparation and retinal explant culture

The retroviral constructs were prepared and purified as previously outlined (Cayouette et al., 2003). Retinal explants were prepared and cultured as previously described (Cayouette et al., 2001). Retroviral infections were carried out after placing the retinal explants in a CO_2 incubator at 37°C 1 h after dissection. In *ex vivo* electroporations and retroviral infections, left and right retinas from the same animal were separated to ensure control and experimental conditions were electroporated between different animals. The clones generated by the retroviral infection were analysed using cell morphology, positioning and cell type markers, as previously described (Elliott et al., 2008).

Western blot

Protein extraction and immunoblotting was carried out as previously described (Ramamurthy et al., 2014). The secondary antibody used was HRP-conjugated goat anti-mouse or HRP-conjugated goat anti-rabbit (1:10,000, Jackson Immunoresearch).

In vivo electroporation

P0 eyes were injected sub-retinally with 3 µg of DNA suspended in 1 µl water containing 0.5% Fast Green and electroporated with 5 pulses at 50 V for 50 ms as previously described (de Melo and Blackshaw, 2011). The mice were sacrificed 14 days or more after the electroporation, and the retinas were dissected, fixed and sectioned as stated above.

CRISPR-Cas9 gRNA generation

CRISPR-Cas9 gRNAs targeting Pou2f1 and Pou2f2 were generated and cloned into pX330-U6-Chimeric_BB-CBh-hSpCas9 vector as described previously (Wang et al., 2014; Cong et al., 2013; Ruan et al., 2017). gRNA sequences used for CRISPR/Cas9 indel knockouts are listed in Table S1.

Plasmids

Pou2f1 and Pou2f2 cDNA were cloned into a pCIG2-IRES-GFP and pCLE-Venus backbone vector using appropriate restriction sites (Lennon et al.,

Development (2020) 147, dev188730. doi:10.1242/dev.188730

1996; Gaiano et al., 2000; Hand et al., 2005). shRNA sequences listed in Table S1 were cloned into pSIREN-retroQ-ZsGreen (Chan et al., 2006). pmNrl-dsRed, pNrl-Pou2f1, pmNrl-Pou2f1, pNrl-Pou2f2 and pmNrl-Pou2f2 were generated by Infusion HD Plus cloning kit using primers listed in Table S1. ThrbPR1:GFP and ThrbPR2:GFP sequences were generated by amplifying the promoter regions of the long and short isoform of Thrb using PCR primers listed in Table S1. PCR products were then cloned into CAG:mGFP in place of the CAG promoter (Matsuda and Cepko, 2007).

EdU labelling assay

EdU (5 µM) was added in the culture medium for 2 h at specified time points, depending on the experiment (see text). A Click-iT EdU Alexa Fluor 647 imaging kit was used to label the cells that incorporated EdU.

Chromatin immunoprecipitation

ChIP was performed using ∼50 E14 retinas per biological replicate (at least three biological replicates were carried out for each ChIP condition). Retinas were dissected and fixed for 10 min with 1% formaldehyde. Glycine/PBS (125 mM) was used to quench the formaldehyde for 10 min. Buffer A [0.25% Triton, 10 mM Tris (pH 8), 10 mM EDTA, 0.5 mM EGTA and protease inhibitors] was added to the samples and incubated for 10 min. The samples were then incubated for 30 min in buffer B [200 mM NaCl, 10 mM Tris (pH 8), 1 mM EDTA, 0.5 mM EGTA and protease inhibitors). The nuclei were sonicated to obtain fragments of 400 bp average length. Immunoprecipitation of the sonicated chromatin was carried out with either mouse IgG (Invitrogen, 02-6502), Pou2f1 (Santa Cruz, 12F11 X) or Pou2f2 (Santa Cruz, F-5 X) whereas 10% of the chromatin was used as input. Dynabeads Protein G (Thermofisher Scientific, 10003D) were used to collect immunoprecipitated material and Qiagen PCR purification kit (28104) was used to isolate DNA fragments after washing and de-crosslinking. qPCR was used to amplify regions of interest using specific primers. A complete primer list is provided in Table S1.

RNA isolation and quantitative PCR

Retinal explants and cKO eyes were dissociated with 100 units of papain (Worthington, LS003124). A MoFlo (Beckman Coulter) cell sorter was used to isolate GFP^+ cells from the electroporated and dissociated retinal explants at various time points. Replicates with more than 1000 GFP^+ cells sorted were included in the study. Collected cells were placed directly into Qiagen Buffer RLT plus and RNeasy microkit (Qiagen, 74004) was used to isolate RNA from the cells, according to the manufacturer's protocol but with an additional 2 min of vortex in Buffer RLT. Isolated RNA was reverse transcribed using Superscript VILO Master Mix (Thermofisher Scientific, 11755050). cDNA was amplified by quantitative PCR using SYBR Green Master mix (Thermofisher Scientific, A25742). The detailed primer list can be found in Table S1 (Ouimette et al., 2010; Emerson et al., 2013). All primers used in this study were validated with a standard curve dilution of cDNA before the experiments were conducted.

Statistical and quantitative analysis

A two-tailed unpaired Student's *t*-test, a one-way ANOVA with Tukey and Dunnett, a two-way ANOVA with Tukey and Mann–Whitney tests were conducted in this study, as indicated in the figure legends. All quantifications shown are mean±s.e.m. *n* represents number of biological replicates. In retroviral clonal analysis, explants containing fewer than 70 GFP^+ clones were pooled to generate a single *n* to obtain representative sampling of the data, as suggested by Pounds and Dyer (2008). In the E14 and P0 retinal explant cultures, samples with disorganised retinal layers were discarded and only retinal explants with organised layers were analysed. Retinal explants with low number of cells counted were pooled to generate one biological replicate. All experiments were repeated at least three times. All retinal sections were oriented according to standard conventions with apical side of the retina at the top of the image. All samples met the power testing criteria of at least $n=3$ with prespecified effect size of a 20% difference with default power value of 0.8 and a significance of $P \leq 0.05$.

αPax6-Cre^+ $Pou2f2^{fl/fl}$ were analysed as follows. Two sections spanning the naso-dorsal and temporo-dorsal regions around 200 µm apart from each other were analysed per marker per animal (four sections per antibody per animal for Lim1). Given that Cre expression in RPCs is restricted to the periphery, only the distal-most one-third of the section was counted. The same region was counted between different animals, sectioned at the same time with the same orientation with the control sections on the same slide. Cells positive for the respective markers were counted in a 200 µm segment on the section. Retinas with poor antibody staining were excluded from the study. The raw counts were then averaged and compared with the wild type from the same experiment. *n* is equal to biological repeats. Cell counts were carried out blind to the genotype; counts for the Pax6 cKO were validated by another lab member who analysed blindly the images taken by the primary investigator. Sections with poor antibody immunostainings were omitted from the analysis.

Chx10-Cre^{ERT2} $Pou2f2^{fl/fl}$ pregnant females were injected with 3 µl/g tamoxifen at E11.5 and sacrificed at E17.5. The embryos were decapitated, and heads were fixed with 4% PFA for 15 min and 1 h depending on the antibody, whereas the tails were used for genotyping. Heads were oriented similarly, and each mutant was embedded in OCT and subsequently cryosectioned together with a control on the same slide. Counts for $Rxrg^-$ and Nrl^- cells were made on two 200 µm segments from the temporal and nasal region of each peripheral retina, averaged and normalised over the control. The investigator was blinded to the genotype during the acquisition of the images and cell counting. Sections with poor antibody immunostaining were omitted from the analysis.

Human ESC maintenance and retinal differentiation culture

The human embryonic stem cell line (H9 from Wicell) was maintained as previously described (Gonzalez-Cordero et al., 2017). For retinal organoid differentiation human ES cells were maintained until 90-95% confluent, then media without FGF (E6, Thermo Fisher) was added to the cultures for 2 days (D1 and 2 of differentiation) followed by a neural induction period (up to 7 weeks) in proneural induction media (Advanced DMEM/F12, MEM non-essential amino acids, N2 Supplement, 100 mM glutamine and penicillin/streptomycin). Lightly pigmented islands of retinal pigmented epithelium (RPE) appeared as early as week 3 in culture. Optic vesicles were formed from within the RPE region between weeks 4 and 7. During this period, neuroretinal vesicles were manually excised with 21 G needles and kept individually in low-binding 96-well plates in retinal differentiation media (DMEM, F12, penicillin/streptomycin and B27 without retinoic acid). At 6 weeks of differentiation, retinal differentiation medium was supplemented with 10% FBS, 100 µM taurine (Sigma, T4871) and 2 mM glutamax, and at 10 weeks 1 µM retinoic acid (RA) was added. For long-term cultures, vesicles were transferred to low-binding 24-well plates (5 vesicles/well) at 10 weeks. At 12 weeks of differentiation, in addition to B27 and other factors described above, media were supplemented with 1% N2 and the RA concentration was reduced to 0.5 µM. Maintenance cultures of hPSCs were fed daily and differentiation cultures were fed every 2 days.

Acknowledgements

We thank Christine Jolicoeur, Jessica Barthe, Marie-Claude Lavallée, Caroline Dubé, Androne Constantin, Odile Neyret-Djossou, Éric Massicotte, Philip St-Onge and Julie Lord for animal and technical assistance. We also thank Pedro Dos Santos França for help with blind quantification of cone numbers in cKO mice and members of the Cayouette lab for their support. We also thank Dr Rachel Pearson for providing Chrnb4-eGFP mouse retinas.

Competing interests

The authors declare no competing or financial interests.

Author contributions

Conceptualization: A.J., P.M., M.C.; Methodology: A.J., P.M., M.C.; Formal analysis: A.J., P.M.; Investigation: A.J., P.M., S.L., K.K., M.K., A.G.-C.; Resources: R.B., R.R.A., M.C.; Writing - original draft: A.J.; Writing - review & editing: P.M., R.B., R.R.A., M.C.; Supervision: R.B., R.R.A., M.C.; Project administration: R.B., R.R.A., M.C.; Funding acquisition: R.B., R.R.A., M.C.

Funding

This work was funded by grants from the Canadian Institutes of Health Research (FDN-159936) and Fighting Blindness Canada (to M.C.), the Fondation Brain Canada/Krembril Foundation (to M.C. and R.B.), as well as the UK Medical

Research Council, the European Research Council and RP Fighting Blindness (to R.A.). A.J. holds a PhD scholarship from Fonds de Recherche du Québec – Santé. M.C. is an Emeritus Scholar from the Fonds de Recherche du Québec – Santé and holds the Gaëtane and Roland Pillenière Chair in Retina Biology from the Institut de recherches cliniques de Montréal Foundation.

Supplementary information

Supplementary information available online at
https://dev.biologists.org/lookup/doi/10.1242/dev.188730.supplemental

Peer review history

The peer review history is available online at
https://dev.biologists.org/lookup/doi/10.1242/dev.188730.reviewer-comments.pdf

References

Akimoto, M., Cheng, H., Zhu, D., Brzezinski, J. A., Khanna, R., Filippova, E., Oh, E. C. T., Jing, Y., Linares, J.-L., Brooks, M. et al. (2006). Targeting of GFP to newborn rods by Nrl promoter and temporal expression profiling of flow-sorted photoreceptors. *Proc. Natl. Acad. Sci. USA* **103**, 3890-3895. doi:10.1073/pnas.0508214103

Aldiri, I., Xu, B., Wang, L., Chen, X., Hiler, D., Griffiths, L., Valentine, M., Shirinifard, A., Thiagarajan, S., Sablauer, A. et al. (2017). The dynamic epigenetic landscape of the retina during development, reprogramming, and tumorigenesis. *Neuron* **94**, 550-568.e10. doi:10.1016/j.neuron.2017.04.022

Altschul, S. F., Gish, W., Miller, W., Myers, E. W. and Lipman, D. J. (1990). Basic local alignment search tool. *J. Mol. Biol.* **215**, 403-410. doi:10.1016/S0022-2836(05)80360-2

Applebury, M. L., Farhangfar, F., Glösmann, M., Hashimoto, K., Kage, K., Robbins, J. T., Shibusawa, N., Wondisford, F. E. and Zhang, H. (2007). Transient expression of thyroid hormone nuclear receptor TRβ2 sets S opsin patterning during cone photoreceptor genesis. *Dev. Dyn.* **236**, 1203-1212. doi:10.1002/dvdy.21155

Bassett, E. A. and Wallace, V. A. (2012). Cell fate determination in the vertebrate retina. *Trends Neurosci.* **35**, 565-573. doi:10.1016/j.tins.2012.05.004

Belliveau, M. J. and Cepko, C. L. (1999). Extrinsic and intrinsic factors control the genesis of amacrine and cone cells in the rat retina. *Development* **126**, 555-566.

Brody, T. and Odenwald, W. F. (2000). Programmed transformations in neuroblast gene expression during Drosophila CNS lineage development. *Dev. Biol.* **226**, 34-44. doi:10.1006/dbio.2000.9829

Carter-Dawson, L. D. and Lavail, M. M. (1979a). Rods and cones in the mouse retina. I. Structural analysis using light and electron microscopy. *J. Comp. Neurol.* **188**, 245-262. doi:10.1002/cne.901880204

Carter-Dawson, L. D. and Lavail, M. M. (1979b). Rods and cones in the mouse retina. II. Autoradiographic analysis of cell generation using tritiated thymidine. *J. Comp. Neurol.* **188**, 263-272.

Cayouette, M., Whitmore, A. V., Jeffery, G. and Raff, M. (2001). Asymmetric segregation of Numb in retinal development and the influence of the pigmented epithelium. *J. Neurosci.* **21**, 5643-5651. doi:10.1523/JNEUROSCI.21-15-05643.2001

Cayouette, M., Barres, B. A. and Raff, M. (2003). Importance of intrinsic mechanisms in cell fate decisions in the developing rat retina. *Neuron* **40**, 897-904. doi:10.1016/S0896-6273(03)00756-6

Cepko, C. L. (1999). The roles of intrinsic and extrinsic cues and bHLH genes in the determination of retinal cell fates. *Curr. Opin. Neurobiol.* **9**, 37-46. doi:10.1016/S0959-4388(99)80005-1

Chan, J. R., Jolicoeur, C., Yamauchi, J., Elliott, J., Fawcett, J. P., Ng, B. K. and Cayouette, M. (2006). The polarity protein Par-3 directly interacts with p75NTR to regulate myelination. *Science* **314**, 832-836. doi:10.1126/science.1134069

Clark, B. S., Stein-O'brien, G. L., Shiau, F., Cannon, G. H., Davis-Marcisak, E., Sherman, T., Santiago, C. P., Hoang, T. V., Rajaii, F., James-Esposito, R. E. et al. (2019). Single-cell RNA-seq analysis of retinal development identifies NFI factors as regulating mitotic exit and late-born cell specification. *Neuron* **102**, 1111-1126.e5. doi:10.1016/j.neuron.2019.04.010

Cleary, M. D. and Doe, C. Q. (2006). Regulation of neuroblast competence: multiple temporal identity factors specify distinct neuronal fates within a single early competence window. *Genes Dev.* **20**, 429-434. doi:10.1101/gad.1382206

Cong, L., Ran, F. A., Cox, D., Lin, S., Barretto, R., Habib, N., Hsu, P. D., Wu, X., Jiang, W., Marraffini, L. A. et al. (2013). Multiplex genome engineering using CRISPR/Cas systems. *Science* **339**, 819-823. doi:10.1126/science.1231143

Daum, J. M., Keles, O., Holwerda, S. J., Kohler, H., Rijli, F. M., Stadler, M. and Roska, B. (2017). The formation of the light-sensing compartment of cone photoreceptors coincides with a transcriptional switch. *eLife* **6**, e31437. doi:10.7554/eLife.31437

de Melo, J. and Blackshaw, S. (2011). In vivo electroporation of developing mouse retina. *J. Vis. Exp.* **52**, 2847. doi:/10.3791/2847

Decembrini, S., Martin, C., Sennlaub, F., Chemtob, S., Biel, M., Samardzija, M., Moulin, A., Behar-Cohen, F. and Arsenijevic, Y. (2017). Cone genesis tracing by the Chrnb4-EGFP mouse line: evidences of cellular material fusion after cone precursor transplantation. *Mol. Ther.* **25**, 634-653. doi:10.1016/j.ymthe.2016.12.015

Doe, C. Q. (2017). Temporal patterning in the Drosophila CNS. *Annu. Rev. Cell Dev. Biol.* **33**, 219-240. doi:10.1146/annurev-cellbio-111315-125210

Donner, A. L., Episkopou, V. and Maas, R. L. (2007). Sox2 and Pou2f1 interact to control lens and olfactory placode development. *Dev. Biol.* **303**, 784-799. doi:10.1016/j.ydbio.2006.10.047

Ebisuya, M. and Briscoe, J. (2018). What does time mean in development? *Development* **145**, dev164368. doi:10.1242/dev.164368

Elliott, J., Jolicoeur, C., Ramamurthy, V. and Cayouette, M. (2008). Ikaros confers early temporal competence to mouse retinal progenitor cells. *Neuron* **60**, 26-39. doi:10.1016/j.neuron.2008.08.008

Emerson, M. M., Surzenko, N., Goetz, J. J., Trimarchi, J. and Cepko, C. L. (2013). Otx2 and Onecut1 promote the fates of cone photoreceptors and horizontal cells and repress rod photoreceptors. *Dev. Cell* **26**, 59-72. doi:10.1016/j.devcel.2013.06.005

Erclik, T., Li, X., Courgeon, M., Bertet, C., Chen, Z., Baumert, R., Ng, J., Koo, C., Arain, U., Behnia, R. et al. (2017). Integration of temporal and spatial patterning generates neural diversity. *Nature* **541**, 365-370. doi:10.1038/nature20794

Gaiano, N., Nye, J. S. and Fishell, G. (2000). Radial glial identity is promoted by Notch1 signaling in the murine forebrain. *Neuron* **26**, 395-404. doi:10.1016/S0896-6273(00)81172-1

Gomes, F. L. A. F., Zhang, G., Carbonell, F., Correa, J. A., Harris, W. A., Simons, B. D. and Cayouette, M. (2011). Reconstruction of rat retinal progenitor cell lineages in vitro reveals a surprising degree of stochasticity in cell fate decisions. *Development* **138**, 227-235. doi:10.1242/dev.059683

Gonzalez-Cordero, A., Kruczek, K., Naeem, A., Fernando, M., Kloc, M., Ribeiro, J., Goh, D., Duran, Y., Blackford, S. J. I., Abelleira-Hervas, L. et al. (2017). Recapitulation of human retinal development from human pluripotent stem cells generates transplantable populations of cone photoreceptors. *Stem Cell Rep.* **9**, 820-837. doi:10.1016/j.stemcr.2017.07.022

Grosskortenhaus, R., Pearson, B. J., Marusich, A. and Doe, C. Q. (2005). Regulation of temporal identity transitions in Drosophila neuroblasts. *Dev. Cell* **8**, 193-202. doi:10.1016/j.devcel.2004.11.019

Grosskortenhaus, R., Robinson, K. J. and Doe, C. Q. (2006). Pdm and Castor specify late-born motor neuron identity in the NB7-1 lineage. *Genes Dev.* **20**, 2618-2627. doi:10.1101/gad.1445306

Hafler, B. P., Surzenko, N., Beier, K. T., Punzo, C., Trimarchi, J. M., Kong, J. H. and Cepko, C. L. (2012). Transcription factor Olig2 defines subpopulations of retinal progenitor cells biased toward specific cell fates. *Proc. Natl. Acad. Sci. USA* **109**, 7882-7887. doi:10.1073/pnas.1203138109

Hand, R., Bortone, D., Mattar, P., Nguyen, L., Heng, J. I.-T., Guerrier, S., Boutt, E., Peters, E., Barnes, A. P., Parras, C. et al. (2005). Phosphorylation of Neurogenin2 specifies the migration properties and the dendritic morphology of pyramidal neurons in the neocortex. *Neuron* **48**, 45-62. doi:10.1016/j.neuron.2005.08.032

Harris, A., Masgutova, G., Collin, A., Toch, M., Hidalgo-Figueroa, M., Jacob, B., Corcoran, L. M., Francius, C. and Clotman, F. (2019). Onecut factors and Pou2f2 regulate the distribution of V2 interneurons in the mouse developing spinal cord. *Front Cell Neurosci.* **13**, 184. doi:10.3389/fncel.2019.00184

He, X., Treacy, M. N., Simmons, D. M., Ingraham, H. A., Swanson, L. W. and Rosenfeld, M. G. (1989). Expression of a large family of POU-domain regulatory genes in mammalian brain development. *Nature* **340**, 35-42. doi:10.1038/340035a0

Hodson, D. J., Shaffer, A. L., Xiao, W., Wright, G. W., Schmitz, R., Phelan, J. D., Yang, Y., Webster, D. E., Rui, L., Kohlhammer, H. et al. (2016). Regulation of normal B-cell differentiation and malignant B-cell survival by OCT2. *Proc. Natl. Acad. Sci. USA* **113**, E2039-E2046. doi:10.1073/pnas.1600557113

Hoshino, A., Ratnapriya, R., Brooks, M. J., Chaitankar, V., Wilken, M. S., Zhang, C., Starostik, M. R., Gieser, L., LA Torre, A., Nishio, M. et al. (2017). Molecular anatomy of the developing human retina. *Dev. Cell* **43**, 763-779.e4. doi:10.1016/j.devcel.2017.10.029

Isshiki, T., Pearson, B., Holbrook, S. and Doe, C. Q. (2001). Drosophila neuroblasts sequentially express transcription factors which specify the temporal identity of their neuronal progeny. *Cell* **106**, 511-521. doi:10.1016/S0092-8674(01)00465-2

Jessell, T. M. (2000). Neuronal specification in the spinal cord: inductive signals and transcriptional codes. *Nat. Rev. Genet.* **1**, 20-29. doi:10.1038/35049541

Kambadur, R., Koizumi, K., Stivers, C., Nagle, J., Poole, S. J. and Odenwald, W. F. (1998). Regulation of POU genes by castor and hunchback establishes layered compartments in the Drosophila CNS. *Genes Dev.* **12**, 246-260. doi:10.1101/gad.12.2.246

Kautzmann, M. A., Kim, D. S., Felder-Schmittbuhl, M. P. and Swaroop, A. (2011). Combinatorial regulation of photoreceptor differentiation factor, neural retina leucine zipper gene Nrl, revealed by in vivo promoter analysis. *J. Biol. Chem.* **286**, 28247-28255. doi:10.1074/jbc.M111.257246

Kim, J., Wu, H. H., Lander, A. D., Lyons, K. M., Matzuk, M. M. and Calof, A. L. (2005). GDF11 controls the timing of progenitor cell competence in developing retina. *Science* **308**, 1927-1930. doi:10.1126/science.1110175

Kiyota, T., Kato, A., Altmann, C. R. and Kato, Y. (2008). The POU homeobox protein Oct-1 regulates radial glia formation downstream of Notch signaling. *Dev. Biol.* **315**, 579-592. doi:10.1016/j.ydbio.2007.12.013
Kohwi, M. and Doe, C. Q. (2013). Temporal fate specification and neural progenitor competence during development. *Nat. Rev. Neurosci.* **14**, 823-838. doi:10.1038/nrn3618
Konig, H., Pfisterer, P., Corcoran, L. M. and Wirth, T. (1995). Identification of CD36 as the first gene dependent on the B-cell differentiation factor Oct-2. *Genes Dev.* **9**, 1598-1607. doi:10.1101/gad.9.13.1598
Lennon, G., Auffray, C., Polymeropoulos, M. and Soares, M. B. (1996). The I.M.A.G.E. Consortium: an integrated molecular analysis of genomes and their expression. *Genomics* **33**, 151-152. doi:10.1006/geno.1996.0177
Li, X., Erclik, T., Bertet, C., Chen, Z., Voutev, R., Venkatesh, S., Morante, J., Celik, A. and Desplan, C. (2013). Temporal patterning of Drosophila medulla neuroblasts controls neural fates. *Nature* **498**, 456-462. doi:10.1038/nature12319
Liu, S., Liu, X., Li, S., Huang, X., Qian, H., Jin, K. and Xiang, M. (2020). Foxn4 is a temporal identity factor conferring mid/late-early retinal competence and involved in retinal synaptogenesis. *Proc. Natl. Acad. Sci.* **117**, 5016-5027. doi:10.1073/pnas.1918628117
Lloyd, A. and Sakonju, S. (1991). Characterization of two Drosophila POU domain genes, related to oct-1 and oct-2, and the regulation of their expression patterns. *Mech. Dev.* **36**, 87-102. doi:10.1016/0925-4773(91)90075-H
Luchina, N. N., Krivega, I. V. and Pankratova, E. V. (2003). Human Oct-1L isoform has tissue-specific expression pattern similar to Oct-2. *Immunol. Lett.* **85**, 237-241. doi:10.1016/S0165-2478(02)00179-7
Ma, L., Cantrup, R., Varrault, A., Colak, D., Klenin, N., Gotz, M., Mcfarlane, S., Journot, L. and Schuurmans, C. (2007). Zac1 functions through TGFbetaII to negatively regulate cell number in the developing retina. *Neural Dev.* **2**, 11. doi:10.1186/1749-8104-2-11
Marquardt, T., Ashery-Padan, R., Andrejewski, N., Scardigli, R., Guillemot, F. and Gruss, P. (2001). Pax6 is required for the multipotent state of retinal progenitor cells. *Cell* **105**, 43-55. doi:10.1016/S0092-8674(01)00295-1
Matsuda, T. and Cepko, C. L. (2007). Controlled expression of transgenes introduced by in vivo electroporation. *Proc. Natl. Acad. Sci. USA* **104**, 1027-1032. doi:10.1073/pnas.0610155104
Mattar, P., Ericson, J., Blackshaw, S. and Cayouette, M. (2015). A conserved regulatory logic controls temporal identity in mouse neural progenitors. *Neuron* **85**, 497-504. doi:10.1016/j.neuron.2014.12.052
Mears, A. J., Kondo, M., Swain, P. K., Takada, Y., Bush, R. A., Saunders, T. L., Sieving, P. A. and Swaroop, A. (2001). Nrl is required for rod photoreceptor development. *Nat. Genet.* **29**, 447-452. doi:10.1038/ng774
Montana, C. L., Lawrence, K. A., Williams, N. L., Tran, N. M., Peng, G.-H., Chen, S. and Corbo, J. C. (2011). Transcriptional regulation of neural retina leucine zipper (Nrl), a photoreceptor cell fate determinant. *J. Biol. Chem.* **286**, 36921-36931. doi:10.1074/jbc.M111.279026
Ng, L., Hurley, J. B., Dierks, B., Srinivas, M., Saltó, C., Vennström, B., Reh, T. A. and Forrest, D. (2001). A thyroid hormone receptor that is required for the development of green cone photoreceptors. *Nat. Genet.* **27**, 94-98. doi:10.1038/83829
Ng, L., Ma, M., Curran, T. and Forrest, D. (2009). Developmental expression of thyroid hormone receptor β2 protein in cone photoreceptors in the mouse. *Neuroreport* **20**, 627-631. doi:10.1097/WNR.0b013e32832a2c63
Novotny, T., Eiselt, R. and Urban, J. (2002). Hunchback is required for the specification of the early sublineage of neuroblast 7-3 in the Drosophila central nervous system. *Development* **129**, 1027-1036.
Oh, E. C. T., Khan, N., Novelli, E., Khanna, H., Strettoi, E. and Swaroop, A. (2007). Transformation of cone precursors to functional rod photoreceptors by bZIP transcription factor NRL. *Proc. Natl. Acad. Sci. USA* **104**, 1679-1684. doi:10.1073/pnas.0605934104
Oh, E. C. T., Cheng, H., Hao, H., Jia, L., Khan, N. W. and Swaroop, A. (2008). Rod differentiation factor NRL activates the expression of nuclear receptor NR2E3 to suppress the development of cone photoreceptors. *Brain Res.* **1236**, 16-29. doi:10.1016/j.brainres.2008.01.028
Ouimette, J.-F., Jolin, M. L., L'honoré, A., Gifuni, A. and Drouin, J. (2010). Divergent transcriptional activities determine limb identity. *Nat. Commun.* **1**, 35. doi:10.1038/ncomms1036
Ozawa, Y., Nakao, K., Shimazaki, T., Shimmura, S., Kurihara, T., Ishida, S., Yoshimura, A., Tsubota, K. and Okano, H. (2007). SOCS3 is required to temporally fine-tune photoreceptor cell differentiation. *Dev. Biol.* **303**, 591-600. doi:10.1016/j.ydbio.2006.11.032
Pearson, B. J. and Doe, C. Q. (2003). Regulation of neuroblast competence in Drosophila. *Nature* **425**, 624-628. doi:10.1038/nature01910
Pounds, S. and Dyer, M. A. (2008). Statistical analysis of data from retroviral clonal experiments in the developing retina. *Brain Res.* **1192**, 178-185. doi:10.1016/j.brainres.2007.08.074
Ramamurthy, V., Jolicoeur, C., Koutroumbas, D., Muhlhans, J., Le, Y.-Z., Hauswirth, W. W., Giessl, A. and Cayouette, M. (2014). Numb regulates the polarized delivery of cyclic nucleotide-gated ion channels in rod photoreceptor cilia. *J. Neurosci.* **34**, 13976-13987. doi:10.1523/JNEUROSCI.1938-14.2014
Rapaport, D. H., Wong, L. L., Wood, E. D., Yasumura, D. and Lavail, M. M. (2004). Timing and topography of cell genesis in the rat retina. *J. Comp. Neurol.* **474**, 304-324. doi:10.1002/cne.20134
Ruan, G.-X., Barry, E., Yu, D., Lukason, M., Cheng, S. H. and Scaria, A. (2017). CRISPR/Cas9-mediated genome editing as a therapeutic approach for leber congenital amaurosis 10. *Mol. Ther.* **25**, 331-341. doi:10.1016/j.ymthe.2016.12.006
Sapkota, D., Chintala, H., Wu, F., Fliesler, S. J., Hu, Z. and Mu, X. (2014). Onecut1 and Onecut2 redundantly regulate early retinal cell fates during development. *Proc. Natl. Acad. Sci. USA* **111**, E4086-E4095. doi:10.1073/pnas.1405354111
Schonemann, M. D., Ryan, A. K., Erkman, L., Mcevilly, R. J., Bermingham, J. and Rosenfeld, M. G. (1998). POU domain factors in neural development. *Adv. Exp. Med. Biol.* **449**, 39-53. doi:10.1007/978-1-4615-4871-3_4
Siegert, S., Scherf, B. G., DEL Punta, K., Didkovsky, N., Heintz, N. and Roska, B. (2009). Genetic address book for retinal cell types. *Nat. Neurosci.* **12**, 1197-1204. doi:10.1038/nn.2370
Suzuki, T., Kaido, M., Takayama, R. and Sato, M. (2013). A temporal mechanism that produces neuronal diversity in the Drosophila visual center. *Dev. Biol.* **380**, 12-24. doi:10.1016/j.ydbio.2013.05.002
Treacy, M. N. and Rosenfeld, M. G. (1992). Expression of a family of POU-domain protein regulatory genes during development of the central nervous system. *Annu. Rev. Neurosci.* **15**, 139-165. doi:10.1146/annurev.ne.15.030192.001035
Turner, D. L., Snyder, E. Y. and Cepko, C. L. (1990). Lineage-independent determination of cell type in the embryonic mouse retina. *Neuron* **4**, 833-845. doi:10.1016/0896-6273(90)90136-4
Wang, S., Sengel, C., Emerson, M. M. and Cepko, C. L. (2014). A gene regulatory network controls the binary fate decision of rod and bipolar cells in the vertebrate retina. *Dev. Cell* **30**, 513-527. doi:10.1016/j.devcel.2014.07.018
Watanabe, T. and Raff, M. C. (1990). Rod photoreceptor development in vitro: intrinsic properties of proliferating neuroepithelial cells change as development proceeds in the rat retina. *Neuron* **4**, 461-467. doi:10.1016/0896-6273(90)90058-N
Young, R. W. (1985a). Cell differentiation in the retina of the mouse. *Anat. Rec.* **212**, 199-205. doi:10.1002/ar.1092120215
Young, R. W. (1985b). Cell proliferation during postnatal development of the retina in the mouse. *Brain Res.* **353**, 229-239. doi:10.1016/0165-3806(85)90211-1
Zelinger, L., Karakülah, G., Chaitankar, V., Kim, J.-W., Yang, H.-J., Brooks, M. J. and Swaroop, A. (2017). Regulation of noncoding transcriptome in developing photoreceptors by Rod differentiation factor NRL. *Invest. Ophthalmol. Vis. Sci.* **58**, 4422-4435. doi:10.1167/iovs.17-21805

Figure S1, Javed et al.

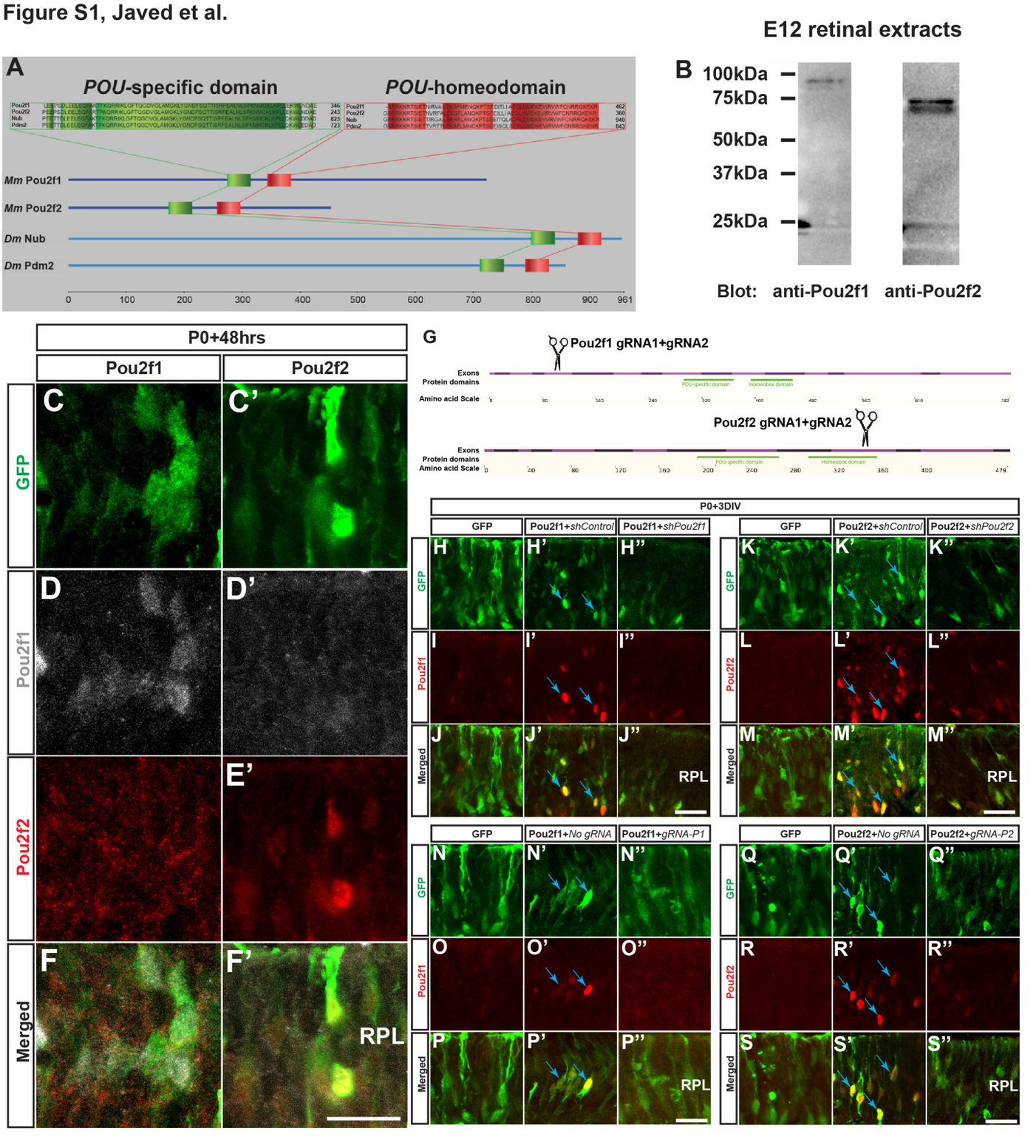

Figure S1: Validation of specific antibodies, shRNA knockdown and CRISPR/Cas9 knockout of Pou2f1/2. (A) Multiple sequence alignment of Drosophila Pdm proteins against mammalian Pou2f1 and Pou2f2 proteins using BLAST-p (Altschul et al., 1990). (B) Western blot of E12 retinal extracts blotted with anti-Pou2f1 and anti-Pou2f2 antibodies. (C-F') Retinal explants electroporated at P0 with Pou2f1-IRES-GFP or Pou2f2-IRES-GFP, cultured for 48hrs, and stained for Pou2f2 (D-D') or Pou2f1 (E-E'). (G) CRISPR-Cas9 gRNA design for Pou2f1 and Pou2f2. (H-M") Retinal explants electroporated at P0 with control GFP (H-M), Pou2f1/Pou2f2 with sh*Control* (H'-M'), or Pou2f1/Pou2f2 with sh*Pou2f1/*sh*Pou2f2* (H''-M''), cultured for 3 days ex-vivo, and stained for Pou2f1 (I-I") or Pou2f2 (L-L"). (N-S") Retinal explants electroporated at P0 with control GFP (N-S), Pou2f1/Pou2f2 with no *gRNA* (N'-S'), or Pou2f1/Pou2f2 with *gRNA-Pou2f1/gRNA-Pou2f2* (N"-S"), cultured for 3 days ex-vivo, and stained for Pou2f1 (O-O") or Pou2f2 (R-R"). (T) Western blot of HEK293T cell lysates either untransfected (-) or transfected (+) with Pou2f1-IRES-GFP alone, Pou2f1-IRES-GFP with shScrambled, or Pou2f1-IRES-GFP with shPou2f1, and blotted using anti-Pou2f1/2 and anti-β-actin antibodies. (V) Western blot of HEK293T cell lysates either un-transfected or transfected with Pou2f2-IRES-GFP with shScrambled or Pou2f2-IRES-GFP with shPou2f2 and blotted using anti-Pou2f1/2 and anti-β-actin antibodies. Scale bars: 10μm.

Figure S2, Javed et al.

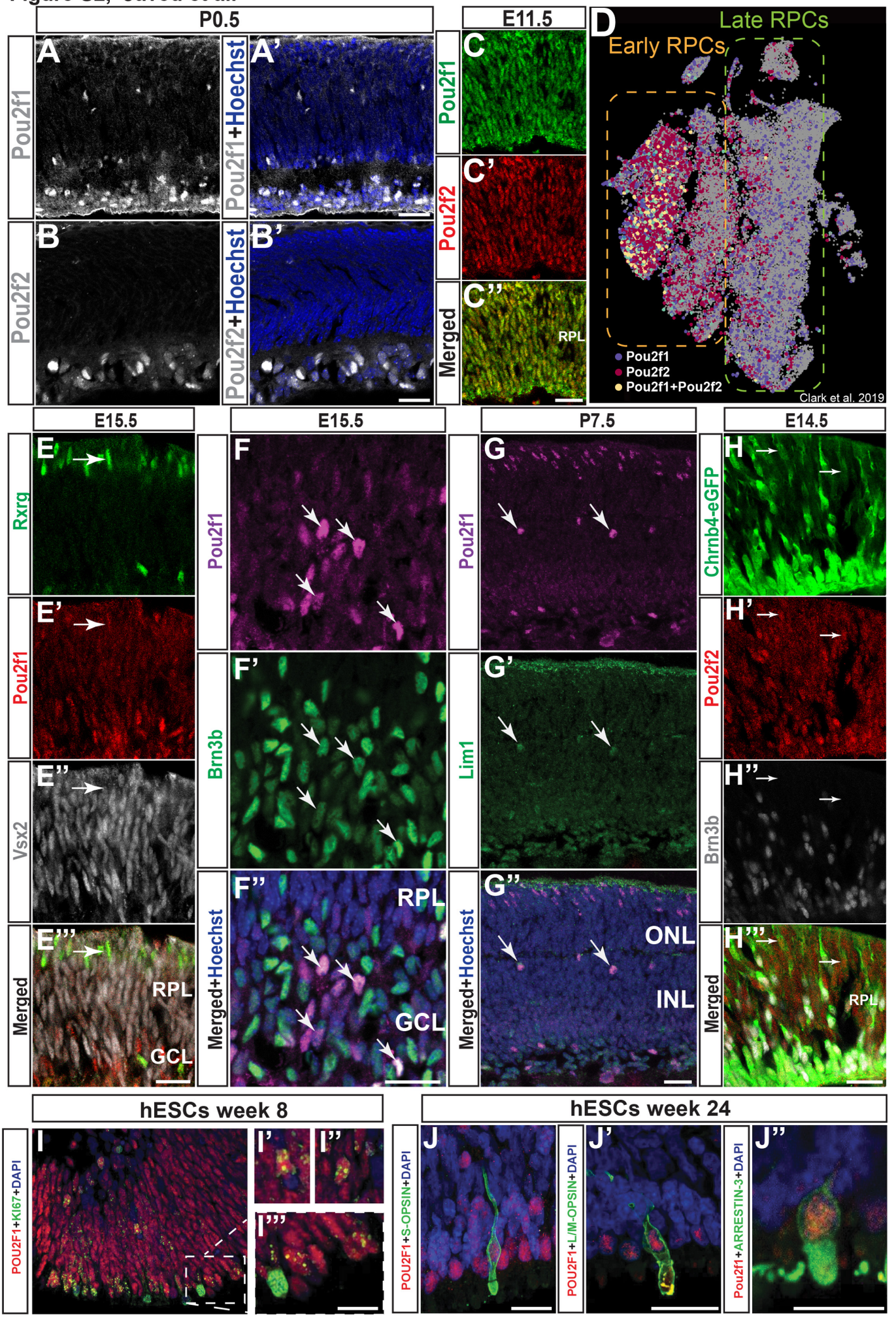

Figure S2: Spatiotemporal expression of Pou2f1 and Pou2f2. (A-B') Immunostaining for Pou2f1 (A) or Pou2f2 (B) in P0.5 mouse retina. (C-C") Immunostaining for Pou2f1 (C) and Pou2f2 (C') in E11.5 mouse retina. (D) scRNA-seq dataset of the developing mouse retina sorted for early and late RPCs. (E-E"') Co-immunostaining of Pou2f1, Rxrg, and Vsx2 in E15.5 mouse retina. Arrows point to Pou2f1^{+ve}Rxrg^{+ve}Chx10^{-ve} cells. (F-G") Immunostaining for Pou2f1, Brn3b or Lim-1 and Hoechst in the mouse retina at E15.5 (F-F") and P7.5 (G-G"). Arrows point to Pou2f1/2^{+ve}Brn3b^{+ve} (F-F") or Pou2f1/2^{+ve}Lim-1^{+ve} (G-G") cells. (H-H"') Co-immustaining of Pou2f2 (H') and Brn3b (H") in Chrnb4-eGFP mouse retina at E14.5. (I-J") Co-immunostaining for POU2F1 and KI67 (I-I"') or S-OPSIN, L/M OPSIN, and ARRESTIN-3 (J-J") in human embryonic stem cell-derived retinal organoids at week 8 or 24, respectively. RPL: Retinal progenitor layer. ONL: Outer nuclear layer. INL: Inner nuclear layer. Scale bars = 20μm (A-C", E-H"'), 10μm (M-N").

Figure S3, Javed et al.

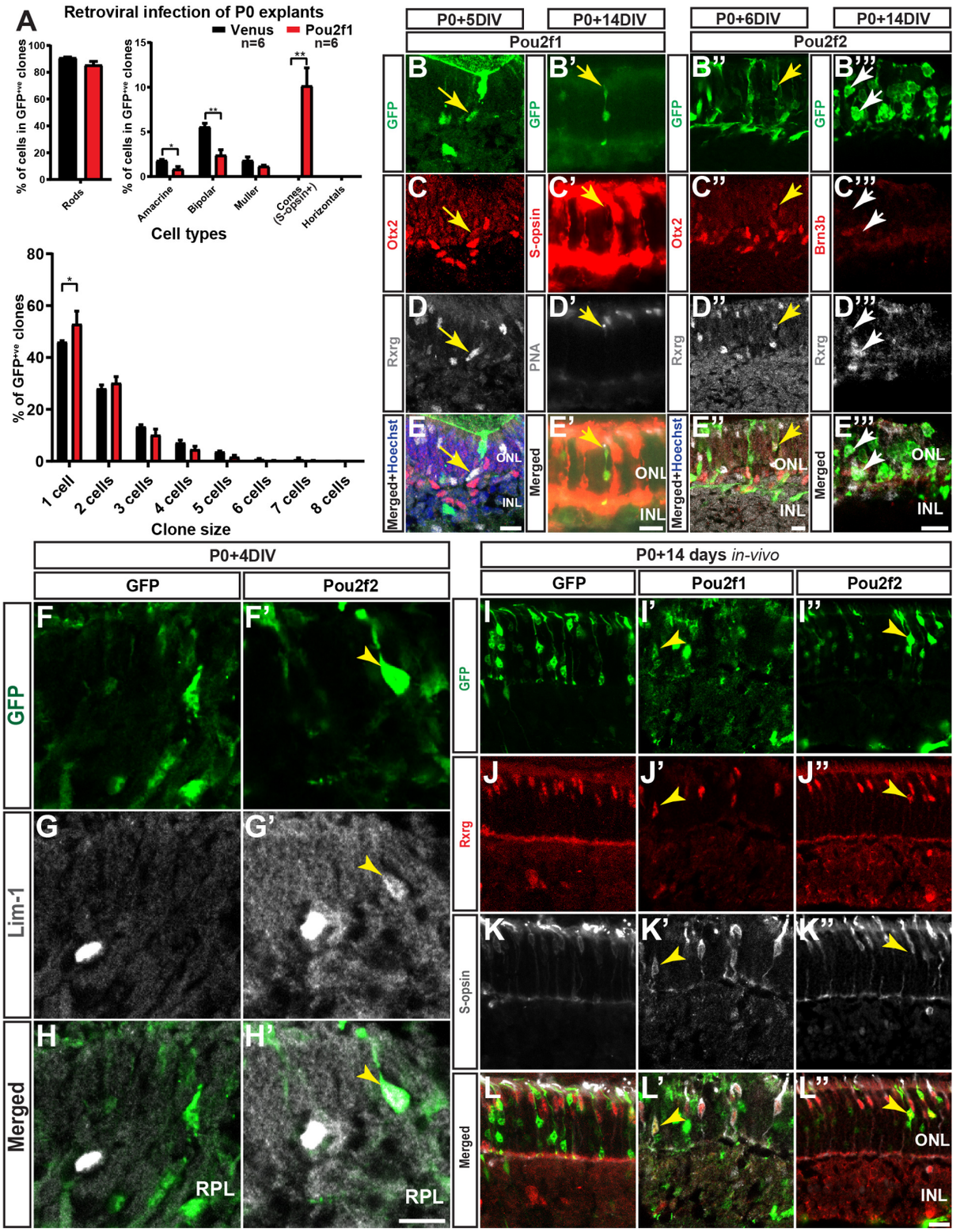

Figure S3: Cone and horizontal cell markers expression after Pou2f1/2 expression in P0 retinal explants. (A) Retinal explants infected with Pou2f1-IRES-Venus at P0, cultured for 14 days, and stained for S-opsin (A') and PNA (A"). (B) Retroviral clonal analysis of Control Venus (1469 clones counted) or Pou2f1 (1055 clones counted) misexpression in mid-late stage retinas. Cell type analysis of GFP^{+ve} cells found in the clones. Cones were counted using S-opsin as a marker, whereas the other cell types were quantified based on morphology and laminar positioning in the retina. Average size distribution of the clones. n values indicated in the graph. (B-E"') Retinal explants either infected with Pou2f1-IRES-Venus (B-B'), cultured for 5 DIV (B) and 14 DIV (B') and stained for Otx2 (C), Rxrg (D), S-opsin (C') or PNA (D') or electroporated with Pou2f2-IRES-GFP (B''-B"'), cultured for 6 DIV (B") and 14 DIV (B"') and stained for Otx2 (C''), Brn3b (C"'), or Rxrg (D"-D"'). Yellow arrows point to co-labelled cells and white arrows point to $GFP^{+ve}Rxrg^{+ve}$ cells lacking Brn3b immunostaining. (F-H') Retinal explants electroporated at P0 with control GFP (F) or Pou2f2-IRES-GFP (F'), cultured for 4 days, and stained for the horizontal cell marker Lim1 (G-G'). Yellow arrowheads point to $GFP^{+ve}Lim\text{-}1^{+ve}$ cells. (I-L") Z-stack projection of electroporated cells with GFP control (I), Pou2f1-IRES-GFP (I'), and Pou2f2-IRES-GFP (I") stained for Rxrg and S-opsin as cone photoreceptor markers. Arrows point to $GFP^{+ve}Rxrg^{+ve}$ cells. ONL: Outer nuclear layer. RPL: Retinal progenitor layer. DIV: Days in-vitro. *$p<0.05$, **$p<0.01$. Statistics: (B) One-way ANOVA with Dunnett for cell types and Two-way ANOVA with Dunnett for clone sizes. Scale bars: 10 μm (B-E"', F-L").

Figure S4, Javed et al.

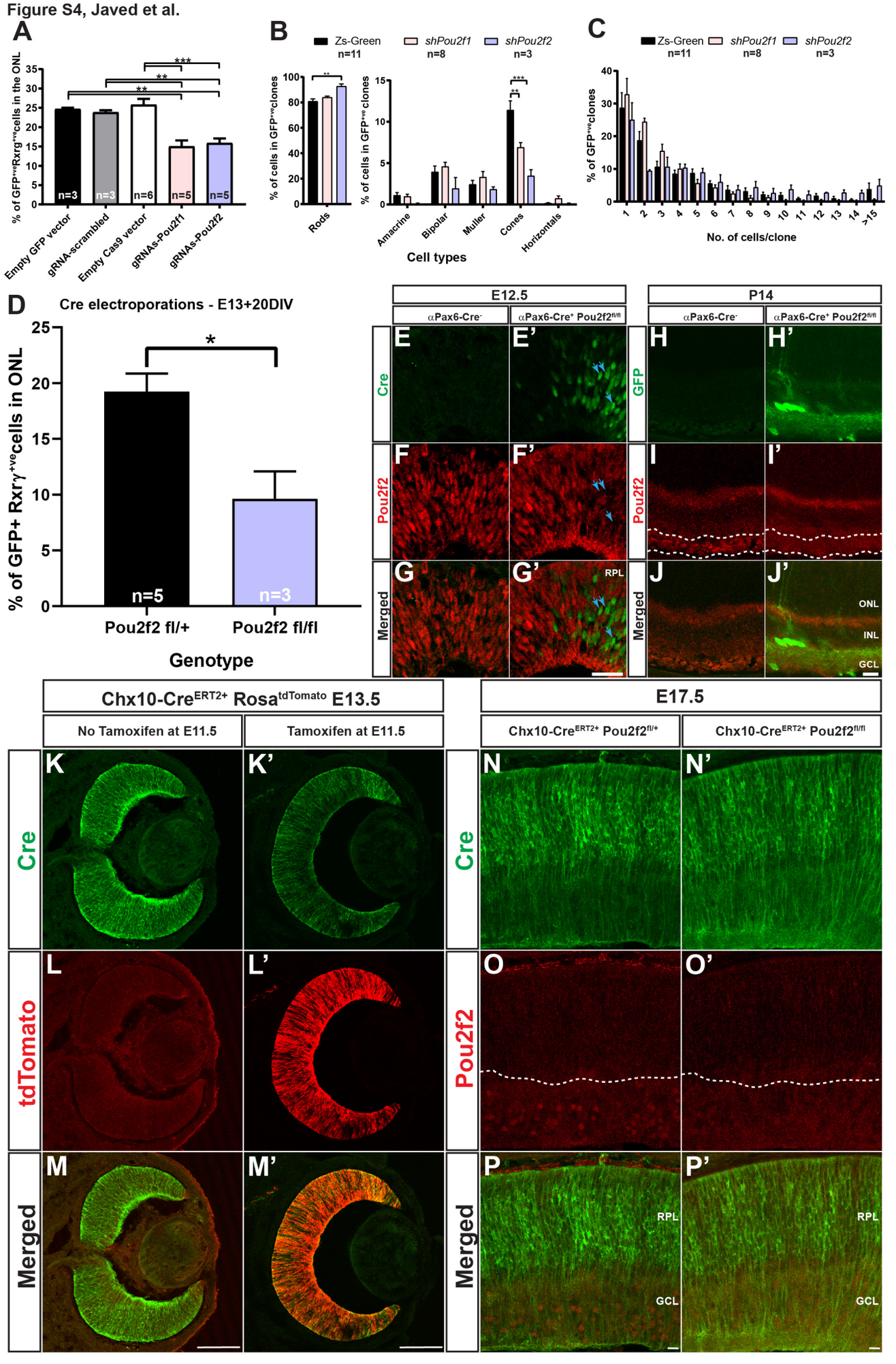

Figure S4: shRNA knockdown, CRISPR/Cas9 knockout and validation of Pou2f2 cKOs. (A) Quantification of the number of $GFP^{+ve}Rxrg^{+ve}$ cells in the outer nuclear layer (ONL) following electroporation of E14 retinal explants with either empty GFP, CRISPR-Cas9-scrambled gRNA with GFP, empty CRISPR-Cas9 with GFP, CRISPR-Cas9-gRNA Pou2f1 with GFP, or CRISPR-Cas9-gRNA Pou2f2 with GFP. (B) Clonal analysis 19 days after infection of E14 retinal explants with retroviral vectors expressing an empty shRNA vector (790 clones counted), or shRNAs for Pou2f1 (619 clones counted) or Pou2f2 (197 clones counted). Cones were counted using Rxrg as a marker whereas other cells were quantified based on morphology and laminar positioning in the retina. (C) Average size distribution of the clones presented in (B). (D) Quantification of the number of $GFP^{+ve}Rxrg^{+ve}$ cells in the ONL following electroporation of retinal explants from E13 $Pou2f2^{fl/+}$ or $Pou2f2^{fl/fl}$ mice with CAG:Cre and cultured for 20 DIV. (E-G') Co-immunostaining of Pou2f2 and Cre in E12.5 αPax6-Cre^{-} (E) or αPax6-Cre^{+} $Pou2f2^{fl/fl}$ (E') mouse retina. Blue arrows show Cre^{+ve} cells lacking Pou2f2 expression. (H-J') Immunostaining of Pou2f2 in P14 retina of αPax6-Cre cKO. Dashed boxes highlight the GCL. (K-M') Immunostaining of Cre and TdTomato in Chx10-Cre^{ERT2+} Rosa26.$tdT^{+/-}$ E13.5 retinas treated without tamoxifen (K) or with tamoxifen (K') at E11.5. (N-P') Co-immunostaining of Cre and Pou2f2 in E17.5 retina of Chx10-Cre cKO. Dashed line highlights the GCL. n values indicated in the graphs. *p<0.05, **p<0.05, ***p<0.05. Statistics: (A, D) Two tailed unpaired t test, (B) One-way ANOVA with Dunnett, (C) Two-way ANOVA with Dunnett. Graphs represent mean±s.e.m. RPL: Retinal progenitor layer, ONL: Outer nuclear layer, INL: Inner nuclear layer, GCL: Ganglion cell layer. Scale bar: 20μm (E-J'), 100μm (K-M'), 10μm (N-P').

Figure S5, Javed et al.

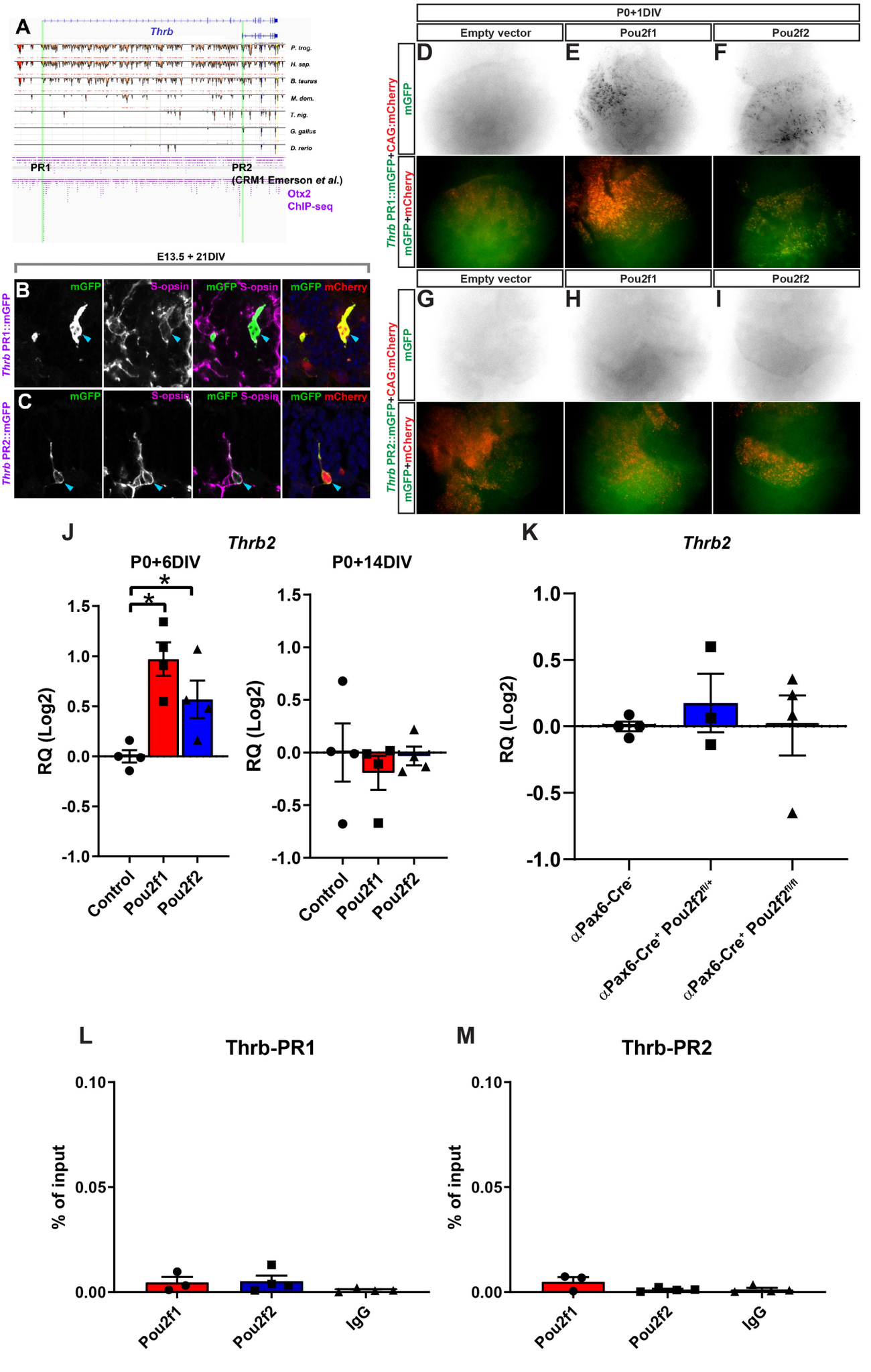

Figure S5: Pou2f1 and Pou2f2 indirectly activate a cis regulatory module of *thrb* active in cones. (A) Sequence alignment of *thrb* gene for different species showing conservation of the cis-regulatory modules (CRM) PR1 and PR2. (B-C) E13 retinal explants co-transfected with *thrbPR1:GFP* (B) or *thrbPR2:GFP* (C) and mCherry, cultured for 21 days, and stained for the cone marker S-opsin. Green arrows point to $GFP^{+ve}mCherry^{+ve}S\text{-}opsin^{+ve}$ cells. (D-I) Photomicrographs of retinal flatmounts electroporated with either control (D, G), Pou2f1 (E, H), or Pou2f2 (F, I) along with either *thrbPR1:GFP* (D-F) or *thrbPR2:GFP* (G-I) and mCherry as a electroporation control at P0 and cultured for one day. (J) RT-qPCR analysis of *Thrb2* from GFP^{+ve} sorted cells 6 days or 14 days after electroporation at P0 of either control GFP (n=4), Pou2f1-IRES-GFP (n=4), or Pou2f2-IRES-GFP (n=4). (K) RT-qPCR analysis *Thrb2* in retinas from P14-P27 $\alpha Pax6\text{-}Cre^{-}$ (n=4), $\alpha Pax6\text{-}Cre^{+}$ $Pou2f2^{fl/+}$ (n=3), or $\alpha Pax6\text{-}Cre^{+}$ $Pou2f2^{fl/fl}$ (n=4) animals. (L-M) Chromatin immunoprecipitation (ChIP) of control IgG (n=4), Pou2f1 (n=3), or Pou2f2 (n=4) followed by quantitative PCR (qPCR) for the *Thrb* promoter region 1 and 2. Statistics: Mann-Whitney test. Graphs represent mean±s.e.m. *$p<0.05$. ONL: Outer nuclear layer. DIV: Days in-vitro. Scale bars: 5μm (B-C), 50μm (D-I).

Figure S6, Javed et al.

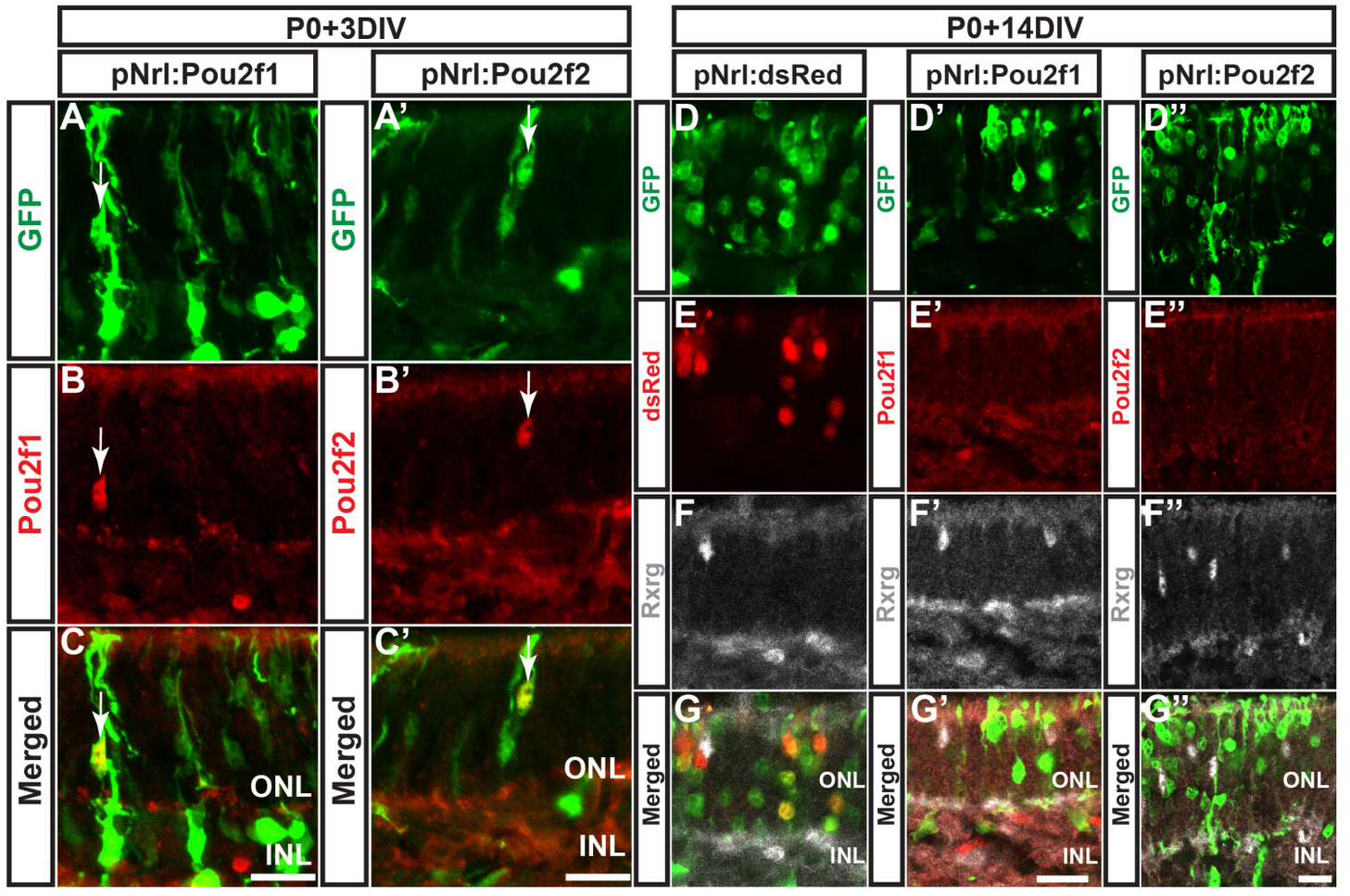

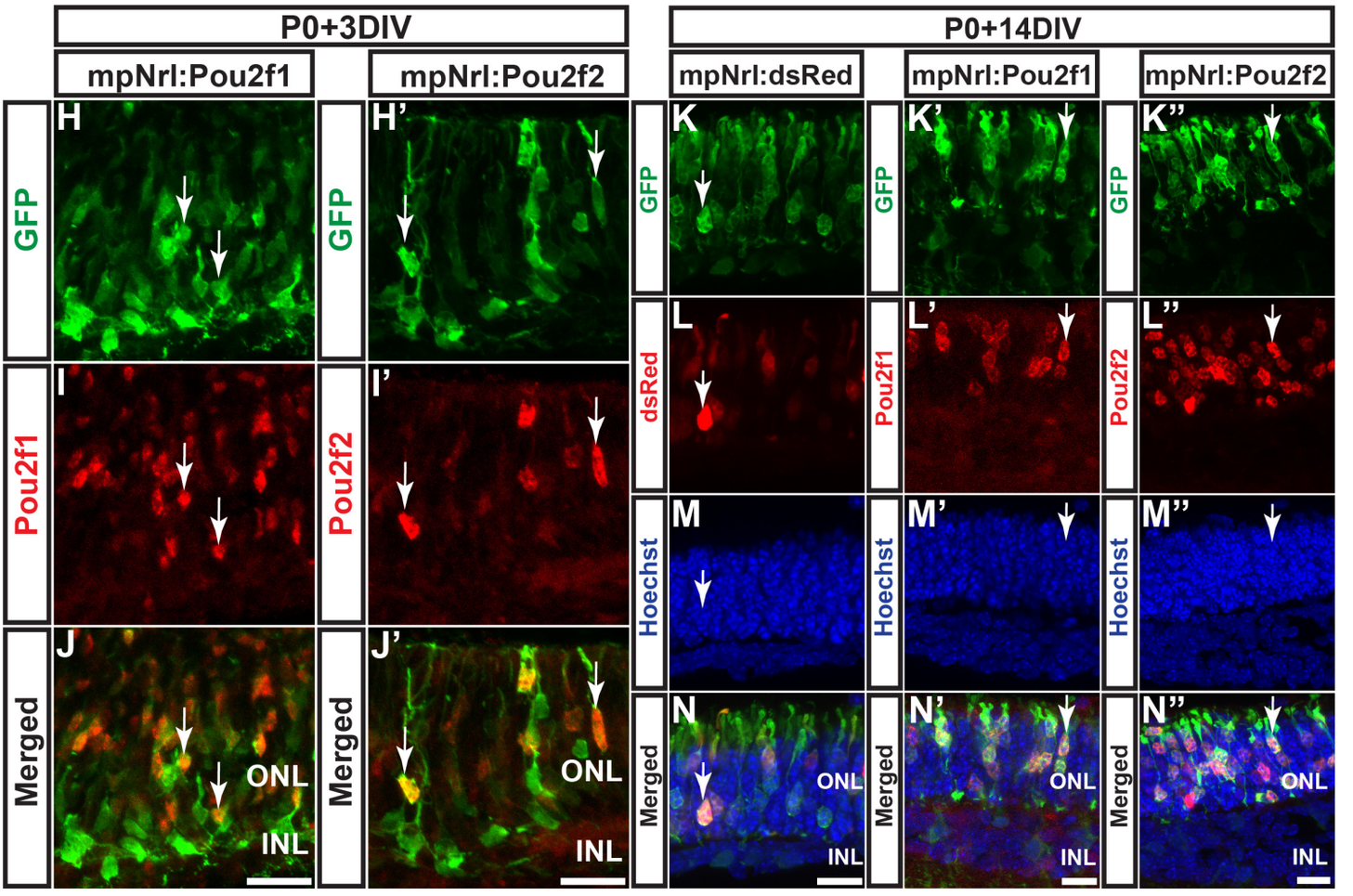

Figure S6: Validation of wildtype and mutated pNrl-Pou2f1/2 vectors. (A-N") Retinal explants electroporated at P0 with either pNrl-Pou2f1/2 (A-G") or pmNrl-Pou2f1/2 (H-N") along with CAG:GFP, cultured for 3DIV (A-C', H-J') or 14DIV (D-G", K-N"), and stained for Pou2f1 (B, E', I, L') or Pou2f2 (B', E", I', L"), Rxrg (F-F") or Hoechst (M-M"). ONL: Outer nuclear layer. INL: Inner nuclear layer. DIV: Days in-vitro. Scale bars: 10 µm (A-N").

Table S1: Sequences of primers and oligos.

Click here to Download Table S1

Table S2 : Materials

Click here to Download Table S2